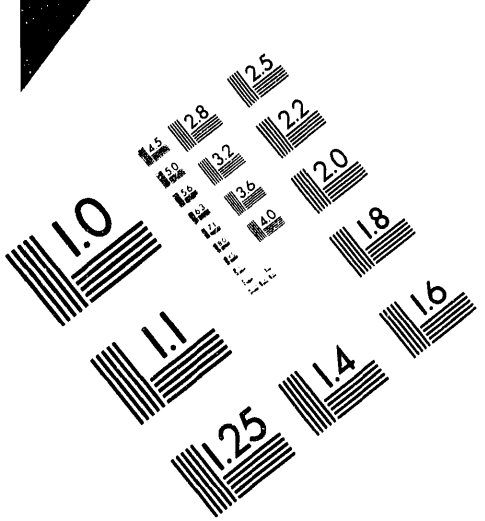

Association for Information and Image Management
1100 Wayne Avenue, Suite 1100
Silver Spring, Maryland 20910
301/587-8202

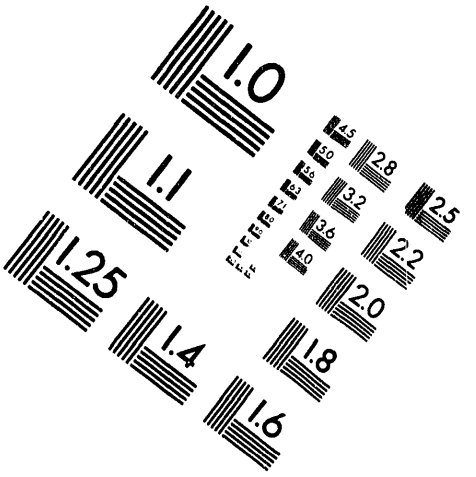

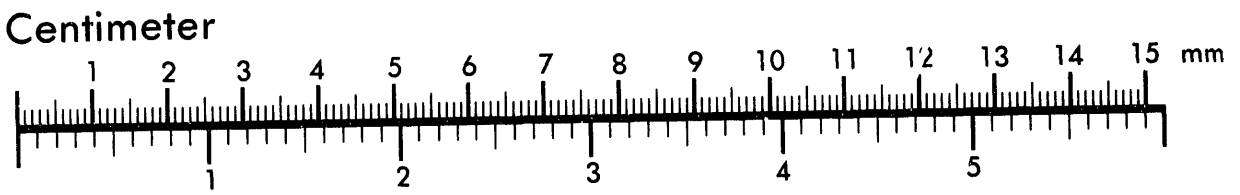

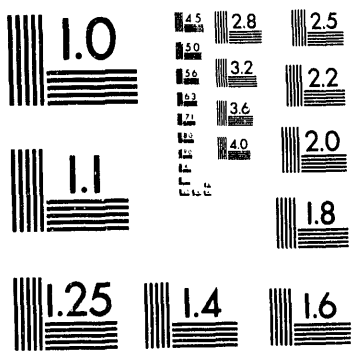

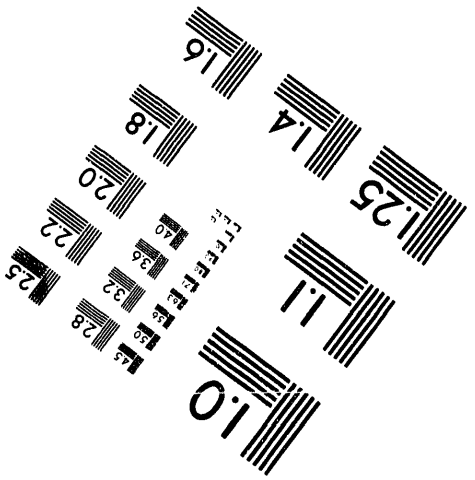

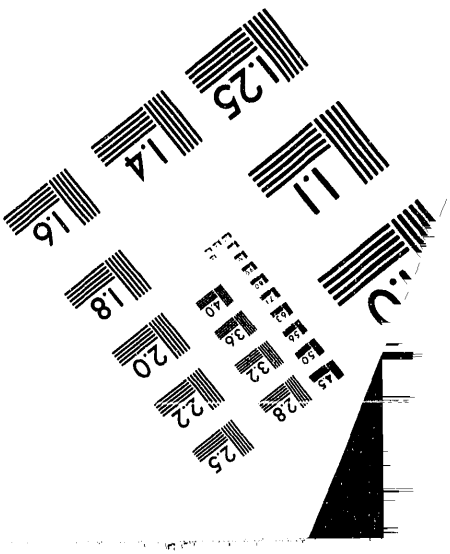

MANUFACTURED TO AIIM STANDARDS
BY APPLIED IMAGE, INC.

1 of 1

NUREG/CR–4744
Vol. 7, No. 2
ANL–93/11
R5

Long-Term Embrittlement of Cast Duplex Stainless Steels in LWR Systems

Semiannual Report
April–September 1992

Manuscript Completed: April 1993
Date Published: July 1993

Prepared by
O. K. Chopra

Argonne National Laboratory
9700 South Cass Avenue
Argonne, IL 60439

Prepared for
Division of Engineering
Office of Nuclear Regulatory Research
U.S. Nuclear Regulatory Commission
Washington, DC 20555
NRC FIN A2243

Previous Documents in Series

Long-Term Embrittlement of Cast Duplex Stainless Steels in LWR Systems: Annual Report, October 1982-September 1983, NUREG/CR-3857, ANL-84-44 (August 1984).

Long-Term Embrittlement of Cast Duplex Stainless Steels in LWR Systems: Annual Report, October 1983-September 1984, NUREG/CR-4204, ANL-85-20 (March 1985).

Long-Term Embrittlement of Cast Duplex Stainless Steels in LWR Systems: Annual Report, October 1984-September 1985, NUREG/CR-4503, ANL-86-3 (January 1986).

Long-Term Embrittlement of Cast Duplex Stainless Steels in LWR Systems: Semiannual Report, October 1985-March 1986, NUREG/CR-4744 Vol. I, No. 1, ANL-86-54 (January 1987).

Long-Term Embrittlement of Cast Duplex Stainless Steels in LWR Systems: Semiannual Report, April-September 1986, NUREG/CR-4744 Vol. I, No. 2, ANL-87-16 (March 1987).

Long-Term Embrittlement of Cast Duplex Stainless Steels in LWR Systems: Semiannual Report, October 1986-March 1987, NUREG/CR-4744, Vol. 2, No. 1, ANL-87-45 (July 1987).

Long-Term Embrittlement of Cast Duplex Stainless Steels in LWR Systems: Semiannual Report, April-September 1987, NUREG/CR-4744, Vol. 2, No. 2, ANL-89/6 (August 1989).

Long-Term Embrittlement of Cast Duplex Stainless Steels in LWR Systems: Semiannual Report, October 1987-March 1988, NUREG/CR-4744, Vol. 3, No. 1, ANL-89/22 (February 1990).

Long-Term Embrittlement of Cast Duplex Stainless Steels in LWR Systems: Semiannual Report, April-September 1988, NUREG/CR-4744, Vol. 3, No. 2, ANL-90/5 (August 1990).

Long-Term Embrittlement of Cast Duplex Stainless Steels in LWR Systems: Semiannual Report, October 1988-March 1989, NUREG/CR-4744, Vol. 4, No. 1, ANL-90/44 (May 1991).

Long-Term Embrittlement of Cast Duplex Stainless Steels in LWR Systems: Semiannual Report, April-September 1989, NUREG/CR-4744, Vol. 4, No. 2, ANL-90/49 (June 1991).

Long-Term Embrittlement of Cast Duplex Stainless Steels in LWR Systems: Semiannual Report, October 1989-March 1990, NUREG/CR-4744, Vol. 5, No. 1, ANL-91/7 (July 1991).

Long-Term Embrittlement of Cast Duplex Stainless Steels in LWR Systems: Semiannual Report, April-September 1990, NUREG/CR-4744, Vol. 5, No. 2, ANL-91/10 (July 1991).

Long-Term Embrittlement of Cast Duplex Stainless Steels in LWR Systems: Semiannual Report, October 1990-March 1991, NUREG/CR-4744, Vol. 6, No. 1, ANL-91/22 (August 1992).

Long-Term Embrittlement of Cast Duplex Stainless Steels in LWR Systems: Semiannual Report, April-September 1991, NUREG/CR-4744, Vol. 6, No. 2, ANL-92/32 (November 1992).

Long-Term Embrittlement of Cast Duplex Stainless Steels in LWR Systems: Semiannual Report, October 1991-March 1992, NUREG/CR-4744, Vol. 7, No. 1, ANL-92/42 (April 1993).

Long-Term Embrittlement of Cast Duplex Stainless Steels in LWR Systems

by

O. K. Chopra

Abstract

This progress report summarizes work performed by Argonne National Laboratory on long-term thermal embrittlement of cast duplex stainless steels in LWR systems during the six months from April-September 1992. A procedure and correlations are presented for predicting Charpy-impact energy, tensile flow stress, fracture toughness J-R curve, tearing modulus, and J_{IC} of aged cast stainless steels from known material information. The "saturation" impact strength and fracture toughness of a specific cast stainless steel, i.e., the minimum value that would be achieved for the material after long-term service, is estimated from the chemical composition of the steel. Mechanical properties as a function of time and temperature of reactor service are estimated from impact energy and flow stress of the unaged material and the kinetics of embrittlement, which are also determined from chemical composition. The J_{IC} values are determined from the estimated J-R curve and flow stress. Examples of estimating mechanical properties of cast stainless steel components during reactor service are presented. A common "lower-bound" J-R curve for cast stainless steels of unknown chemical composition is also defined for a given grade of steel, ferrite content, and temperature.

Contents

List of Figures

List of Tables

Nomenclature

C	Coefficient of the power-law J-R curve.
Cr_{eq}	Chromium equivalent for a material (wt.%).
C_V	Room-temperature "normalized" Charpy-impact energy, i.e., Charpy-impact energy per unit fracture area (J/cm^2).
C_{Vint}	Initial room-temperature "normalized" Charpy-impact energy of an unaged material (J/cm^2).
C_{Vsat}	Room-temperature "normalized" Charpy-impact energy of a material at saturation, i.e., the minimum impact energy that would be achieved for a material after long-term service (J/cm^2).
J_d	Deformation J per ASTM Specification E 813-85 or E 1152-87 (kJ/m^2).
n	Exponent of the power-law J-R curve.
Ni_{eq}	Nickel equivalent for the material (wt.%).
P	Aging parameter, i.e., the log of the time of aging at 400°C.
Q	Activation energy for the process of thermal embrittlement (kJ/mole).
R	Ratio of tensile flow stress of aged, σf_{aged}, and unaged, σf_{unaged}, cast stainless steels.
t	Service or aging time (h).
T_s	Service or aging temperature (°C).
α	Shape factor of the curve for the change in room-temperature Charpy-impact energy with time and temperature of aging.
β	Half the maximum change in room-temperature Charpy-impact energy.
δ_c	Ferrite content calculated from the chemical composition of a material (%).
Δa	Crack extension (mm).
Φ	Material parameter.
θ	Aging behavior at 400°C, i.e., the log of the time to achieve β reduction in impact energy at 400°C.
σ	Standard deviation for the fit to a data set.

SI units of measure have been used in this report. Conversion factors for measurements in British units are as follows:

To convert	to	multiply by
in.	mm	25.4
J*	ft·lb	0.7376
kJ/m^2	$in.-lb/in.^2$	5.71015
kJ/mole	kcal/mole	0.239

* When impact energy is expressed in J/cm^2, first multiply by 0.8 to obtain impact energy of a standard Charpy-V notch specimen in J.

Executive Summary

Cast stainless steels used in pump casings, valve bodies, piping, and other components in coolant systems of light water nuclear reactors (LWRs) suffer a loss in toughness after many years of service at temperatures in the range of 280–320°C (≈536–608°F). A program has been conducted at Argonne National Laboratory (ANL) to investigate the low-temperature thermal embrittlement of cast duplex stainless steels under LWR operating conditions and to evaluate possible remedies for thermal embrittlement problems in existing and future plants. The scope of the investigation included the following goals: (1) characterize and correlate the microstructure of in-service reactor components and laboratory-aged material with loss of fracture toughness to establish the mechanism of aging and validate the simulation of in-reactor degradation by accelerated aging, (2) establish the effects of key compositional and metallurgical variables on the kinetics and extent of thermal embrittlement, and (3) develop the methodology and correlations necessary for predicting the toughness loss suffered by cast stainless steel components during the normal and extended life of LWRs.

Microstructural and mechanical-property data have been obtained on 25 experimental heats (static-cast keel blocks and slabs) and 6 commercial heats (centrifugally cast pipes, a static-cast pump impeller, and a static-cast pump casing ring), as well as on reactor-aged material of CF-3, CF-8, and CF-8M grades of cast stainless steel. The ferrite content of the cast materials ranges from 3 to 30%. Ferrite morphology for castings containing >5% ferrite is either lacy or acicular.

Investigations at ANL and elsewhere have shown that thermal embrittlement of cast stainless steel components can occur during the reactor design lifetime of 40 yr. Thermal aging at reactor temperatures increases the tensile strength and decreases the impact energy and fracture toughness of the steels. The Charpy transition curve shifts to higher temperatures. Different heats exhibit different degrees of thermal embrittlement. The low-C CF-3 steels are the most resistant and the Mo-bearing high-C CF-8M steels the least resistant to thermal embrittlement.

Embrittlement of cast stainless steels results in brittle fracture associated with either cleavage of the ferrite or separation of the ferrite/austenite phase boundary. Thermal aging of cast stainless steels at temperatures <500°C (<932°F) leads to precipitation of additional phases in the ferrite, e.g., formation of a Cr-rich α' phase by spinodal decomposition; nucleation and growth of α'; precipitation of a Ni- and Si-rich G phase, $M_{23}C_6$, and γ_2 (austenite); and additional precipitation and/or growth of existing carbides at the ferrite/austenite phase boundaries. Formation of α' phase provides the strengthening mechanisms that increase strain hardening and local tensile stress. Consequently, the critical stress level for brittle fracture is attained at higher temperatures. Predominantly brittle failure occurs when either the ferrite phase is continuous (e.g., in cast material with a large ferrite content) or the ferrite/austenite phase boundary provides an easy path for crack propagation (e.g., in high-C grades of cast steel with large phase-boundary carbides). Consequently, the amount, size, and distribution of the ferrite phase in the duplex structure, and the presence of phase-boundary carbides are important parameters in controlling the degree or extent of thermal embrittlement.

This is the final progress report in this series. It presents a procedure and correlations for estimating Charpy-impact energy, tensile flow stress, fracture toughness J-R curves, and J_{IC}

values of aged cast stainless steels (ASTM A 351) from known material information. Mechanical properties of a specific cast stainless steel are estimated from the extent and kinetics of thermal embrittlement. Embrittlement of cast stainless steels is characterized in terms of room temperature (RT) Charpy-impact energy. The extent or degree of thermal embrittlement at "saturation," i.e., the minimum impact energy that can be achieved for a material after long-term aging, is determined from the chemical composition of the steel. Charpy-impact energy as a function of time and temperature of reactor service is estimated from the kinetics of thermal embrittlement, which is also determined from the chemical composition. The initial impact energy of the unaged steel is required for these estimations. Initial tensile flow stress is needed for estimating the flow stress of the aged material. The fracture toughness J-R curve for the material is then obtained by correlating RT Charpy-impact energy with fracture toughness parameters. The values of J_{IC} are determined from the estimated J-R curve and flow stress. A common "predicted lower-bound" J-R curve for cast stainless steels with unknown chemical composition is also defined for a given grade of steel, range of ferrite content, and temperature.

1 Introduction

Cast stainless steels used in light water reactor (LWR) systems for primary pressure-boundary components, such as valve bodies, pump casings, and primary coolant piping, are susceptible to thermal embrittlement at reactor operating temperatures, i.e., 280–320°C (536–608°F). Thermal aging of cast stainless steel (i.e., ASTM Specification A-351 Grades* CF-3, CF-3A, CF-8, CF-8A, and CF-8M) at these temperatures increases hardness and tensile strength and decreases ductility, impact strength, and fracture toughness of the steel. The Charpy transition curve shifts to higher temperatures. Investigations at Argonne National Laboratory (ANL)[1-14] and elsewhere[15-22] have shown that thermal embrittlement of cast stainless steel components can occur during the reactor design lifetime of 40 yr.

An assessment of mechanical-property degradation due to thermal embrittlement is, therefore, required to evaluate the continued performance of cast stainless steel components during prolonged exposure to service temperatures, because rupture of the primary pressure boundary could lead to a loss-of-coolant accident and possible exposure of the public to radiation. Thermal embrittlement of cast stainless steel components has been identified in 10 CFR Part 54 of the Code of Federal Regulations as a degradation mechanism that must be addressed in license-renewal applications for LWRs. Thermal embrittlement has been recognized as a major technical issue in several industry reports (IRs), including the IRs for Pressurized Water Reactor Coolant System and Boiling Water Reactor Primary Coolant Pressure Boundary.

The procedure for assessing thermal embrittlement of cast stainless steel is to first identify those components, or regions of a component, that require special attention, and then use a screening criterion by which their suitability for further operation is evaluated. The criterion currently proposed in several IRs is that an assessment of thermal embrittlement is not required when the volume fraction of ferrite is below a specified level. For the components that do not pass the screening criterion, lower-bound fracture properties for thermally aged cast stainless steel are used to perform leak-before-break analyses or critical-flaw-size calculations outlined in ASME Nuclear Code Case N-481. The lower-bound mechanical properties are obtained from data on a heat of material considered representative of the "worst case" for thermal embrittlement.

A program has been conducted at ANL to investigate the significance of low-temperature embrittlement of cast duplex stainless steels under LWR operating conditions. Microstructural and mechanical-property data have been obtained on 25 experimental heats (19 in the form of static-cast keel blocks and 6 in the form of 76-mm slabs) and 6 commercial heats (centrifugally cast pipes and a static-cast pump impeller and pump casing ring),[1-7] as well as on reactor-aged material of Grades CF-3, CF-8, and CF-8M cast stainless steel.[8] Specimen blanks for Charpy-impact, tensile, and J-R curve tests were aged at 290, 320, 350, and 400°C (554, 608, 662, and 752°F) for times up to 58,000 h. Reactor-aged materials were obtained from four check valves, two main shut-off valves, a pump volute of the Shippingport reactor, and from the recirculating-pump cover plate assembly of the KRB reactor in Gundremmingen, Germany. The KRB pump cover plate was in service for ≈8 effective full-power years (efpys) at

* In this report Grades CF-3A and CF-8A are considered equivalent to CF-3 and CF-8, respectively. The A designation represents high tensile strength. The chemical composition of CF-3A and CF-8A are further restricted within the composition limits of CF-3 and CF-8, respectively, to obtain a ferrite/austenite ratio that results in higher ultimate and yield strengths.

284°C (543°F) and the Shippingport components were in service for ≈13 efpys at 281°C (538°F) for the hot leg and 264°C (507°F) for the cold leg. In addition, the Shippingport components were at a hot standby condition for ≈2 yr at 204°C (399°F).

Microstructures of in-service reactor components and laboratory-aged materials were characterized and correlated with loss of fracture toughness to establish the mechanism of aging and validate the simulation of in-reactor degradation by accelerated aging.[12-14] The mechanical-property data base was examined to establish the effects of key compositional and metallurgical variables on the kinetics and extent of thermal embrittlement. The results indicate that assessment of thermal embrittlement of cast stainless steel should be based on the chemical composition of the steel. Assessments based on the proposed delta-ferrite screening criterion must be very conservative or it may not be adequate for some steels, in particular Mo-bearing CF-8M steels. A procedure and correlations have been developed at ANL for estimating mechanical properties of cast stainless steel components under LWR operating conditions from material information readily available in certified material test records (CMTRs).[9] The correlations were later updated and optimized with data on cast stainless steels that were aged up to ≈58,000 h at 290-350°C.[10,11] The results are expressed in terms of engineering fracture toughness parameters that can be used in fitness-for-service analysis.

This is the final progress report in this series. The report describes the procedure and correlations for estimating Charpy-impact, tensile flow stress, and fracture toughness of cast stainless steels during thermal aging in LWRs and discusses the mechanisms of thermal embrittlement. The criteria used in developing these correlations ensure that the estimated mechanical properties are adequately conservative for cast stainless steels defined by ASTM Specification A 351. The correlations do not consider the effects of metallurgical differences that may arise from differences in production heat treatment or casting process and, therefore, may be overly conservative for some steels. Examples of estimating mechanical properties of cast stainless steel components during reactor service are presented. Mechanical properties are expressed in SI units (see Nomenclature for units of measure and for conversion factors for British units).

2 Mechanism of Thermal Embrittlement

Thermal embrittlement of cast duplex stainless steels results in brittle fracture associated with either cleavage of the ferrite or separation of the ferrite/austenite phase boundary (Fig. 1). Thermal aging of cast stainless steels at temperatures <500°C (932°F) leads to precipitation of additional phases in the ferrite, e.g., formation of a Cr-rich α' phase by spinodal decomposition; nucleation and growth of α'; precipitation of a Ni- and Si-rich G phase, $M_{23}C_6$, and γ_2 (austenite); and additional precipitation and/or growth of existing carbides at the ferrite/austenite phase boundaries.[10-14,23-28] Thermal aging has little or no effect on the austenite phase. The formation of Cr-rich regions by spinodal decomposition, the primary strengthening mechanism for ferrite, increases strain hardening and local tensile stress. Consequently, the critical stress level for brittle fracture is achieved at higher temperatures.

The degree or extent of thermal embrittlement is controlled by the amount of brittle fracture. In some cast stainless steels, a fraction of the material may fail in brittle fashion but the surrounding austenite provides ductility and toughness. Such steels have adequate impact strength even after long-term aging. A predominantly brittle failure occurs when either the

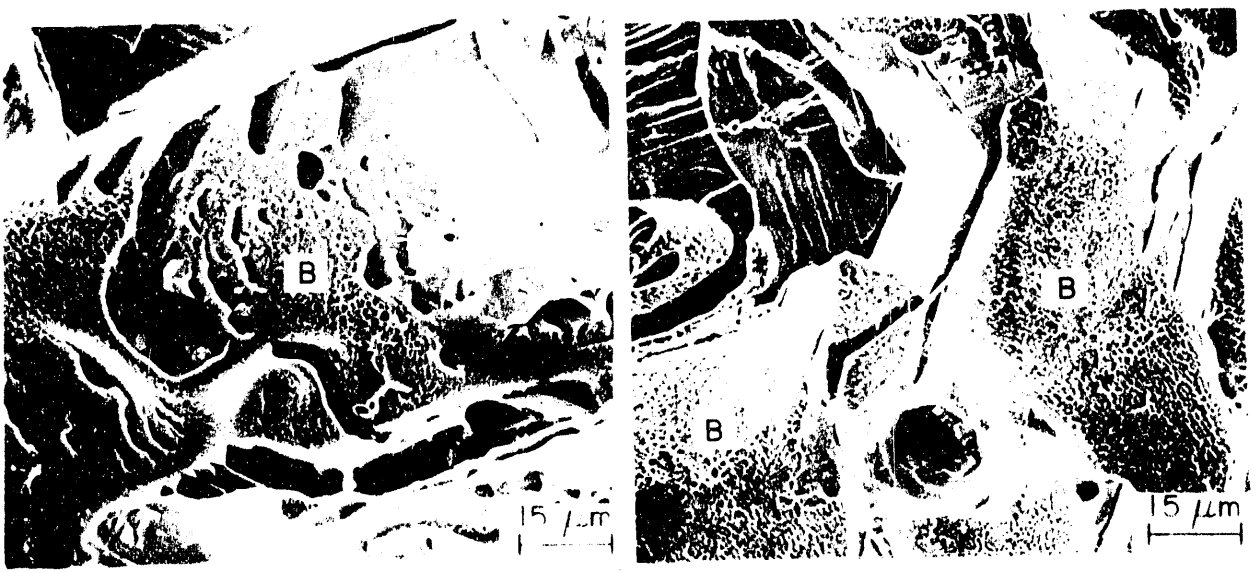

Figure 1. Fracture surface of impact test specimens of unaged CF-8 cast stainless steel tested at -197°C. B = Phase boundary separation.

ferrite phase is continuous, e.g., in cast material with a large ferrite content, or the ferrite/austenite phase boundary provides an easy path for crack propagation, e.g., in high-C or high-N steels that contain phase-boundary carbides or nitrides. Consequently, the amount, size, and distribution of ferrite in the duplex structure and phase-boundary precipitates are important parameters that control the extent of thermal embrittlement. The decrease in Charpy-impact energy during thermal aging at 400°C (752°F) for various heats of cast stainless steel[4-6,15,19,21] is shown in Fig. 2. The results indicate that all the materials reach a "saturation" impact energy, i.e., a minimum value that would be achieved by the material after long-term aging. The actual value of saturation impact energy for a specific cast stainless steel is independent of aging temperature but depends strongly on the chemical composition of the steel; it is lower for the Mo-bearing CF-8M steels than for the Mo-free CF-3 or CF-8 steels, and decreases with an increase in ferrite content or the concentration of C or N in the steel.

The time to reach saturation, i.e., the kinetics of thermal embrittlement, depends on both material and aging parameters. Figure 2 indicates that the time for aging at 400°C for a given decrease in impact energy varies more than 2 orders of magnitude for the various heats, e.g., <1,000 h for the Electric Power Research Institute (EPRI) heat, 1,000-10,000 h for the ANL and Framatome (FRA) heats, and 10,000-30,000 h for the Georg Fischer Co. (GF) heats. Activation energies of thermal embrittlement range from 65 to 230 kJ/mole.[1-6,13-15,17-19,29] These values are well below the 202 kJ/mole value associated with Cr bulk diffusion in the Fe-28Cr alloy.[30] Small changes in the constituent elements of the material can cause the kinetics of thermal embrittlement to vary significantly. The logarithm of the aging time at 400°C for a 50% reduction in Charpy-impact energy has been shown to be an important parameter for characterizing the kinetics of thermal embrittlement.[9] Activation energy is high for steels that show fast embrittlement at 400°C and low for those that show slow embrittlement at 400°C. Also, materials with the same chemical composition but different heat treatment show different kinetics of embrittlement.[15] Microstructural examination of aged cast stainless steels suggests

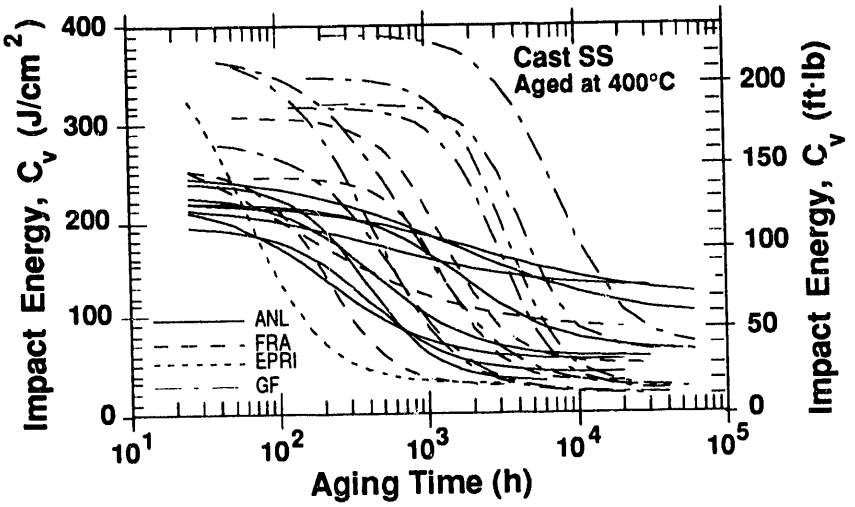

Figure 2. Decrease in Charpy-impact energy for various heats of cast stainless steels aged at 400°C. FRA = Framatome, EPRI = Electric Power Research Institute, GF = Georg Fischer Co.

that slow embrittlement at 400°C and low activation energy are associated with clusters of Ni–Si, Mo–Si, and Ni–Si–Mo in the ferrite matrix.[12-14] These clusters are considered precursors of G-phase nucleation and precipitation. Cast stainless steels with low activation energy and slow embrittlement at 400°C show G-phase precipitation after aging, and steels with high activation energy and fast embrittlement at 400°C do not contain a G phase.[12-14,23,24] The presence of Ni–Si–Mo clusters in the ferrite matrix of an unaged material may be considered a signature of steels that are potentially sensitive to thermal embrittlement, i.e., steels with Ni–Si–Mo clusters in the ferrite matrix show low activation energy for thermal embrittlement.

The kinetics of embrittlement are also influenced by aging temperature. For a specific heat of cast stainless steel, activation energy of thermal embrittlement is not constant over the temperature range of 290–450°C (554–842°F), but increases with decreasing temperature.[1-3,17] The increase is particularly significant between 400 and 450°C; activation energy can be represented by an average value in the temperature range of 290–400°C. In addition, materials aged at 450°C show additional precipitation of phase-boundary carbides (also nitrides in high-N steels) and a decrease in ferrite content of the steel.[1,2] At reactor temperatures, such processes either do not occur or their kinetics are extremely slow. Consequently, data obtained at 450°C aging do not reflect the mechanisms active under reactor operating conditions, and extrapolation of the 450°C data to predict the extent of thermal embrittlement at reactor temperatures is not valid.

The kinetics of thermal embrittlement of cast stainless steels are controlled primarily by the kinetics of ferrite strengthening, e.g., activation energy determined from ferrite hardness measurements shows very good agreement with that obtained from the Charpy-impact data.[17,18,29] Microstructural characterization and annealing studies on thermally aged cast stainless steel show that strengthening of ferrite is caused primarily by spinodal decomposition of ferrite to form Cr-rich α' phase.[4,12,13] Consequently, the kinetics of thermal embrittlement

should be controlled by the amplitude and frequency of Cr fluctuations produced by spinodal decomposition, i.e., by the size and spacing of the α' phase.

The low activation energies of thermal embrittlement are most likely caused by variations in the spacing of Cr fluctuations; atom probe field-ion microscopy studies indicate that the spacing between Cr fluctuations decreases with decreasing temperature.[23,27] During thermal aging, production heat treatment and possibly the casting process, both of which affect ferrite composition and microstructure of unaged material, can influence microstructural evolution and, therefore, the kinetics of embrittlement. As discussed above, G-phase precipitates are always associated with low activation energy of thermal embrittlement.

3 Assessment of Thermal Embrittlement

Mechanical properties of cast stainless steels during service are estimated from the extent of thermal embrittlement of the material. The extent of thermal embrittlement is characterized by room-temperature (RT) "normalized" Charpy-impact energy.* A correlation for the extent of embrittlement at "saturation," i.e., the minimum impact energy that would be achieved for a specific material after long-term aging, is given in terms of chemical composition. The extent of thermal embrittlement as a function of time and temperature of reactor service is estimated from the extent of embrittlement at saturation and from correlations that describe the kinetics of embrittlement, which are also given in terms of the chemical composition of the steel. The fracture toughness J-R curve for a material is then obtained from the correlation between fracture toughness parameters and the RT Charpy-impact energy used to characterize the extent of thermal embrittlement. Tensile flow stress is estimated from initial flow stress of the unaged material and the kinetics of thermal embrittlement.

A flow diagram for estimating mechanical properties of cast stainless steels during reactor service is shown in Fig. 3. The estimation scheme is divided into three sections on the basis of available material information. In Section A of the flow diagram, predicted "lower-bound" fracture toughness and Charpy-impact energy are defined for CF-3, CF-8, and CF-8M steels of unknown composition. When the ferrite content of the steel is known, a different lower-bound fracture toughness and impact energy are defined for steels containing <10%, 10-15%, or >15% ferrite.

Sections B and C of the flow diagram present procedures for estimating mechanical properties when a CMTR is available. Section B describes the estimation of "saturation" impact energy and fracture toughness J-R curve. The only information needed for these estimations is the chemical composition of the material. A screening criterion, may be applied to these saturation values of fracture toughness or Charpy-impact energy to check whether further evaluation of thermal embrittlement is required for the material. Cast stainless steel components with adequate saturation fracture toughness would not require any further assessment of thermal embrittlement.

The correlations presented here account for the degradation of mechanical properties due to thermal aging. They do not explicitly consider the initial fracture properties of the unaged

* Charpy-impact energy per unit fracture area.

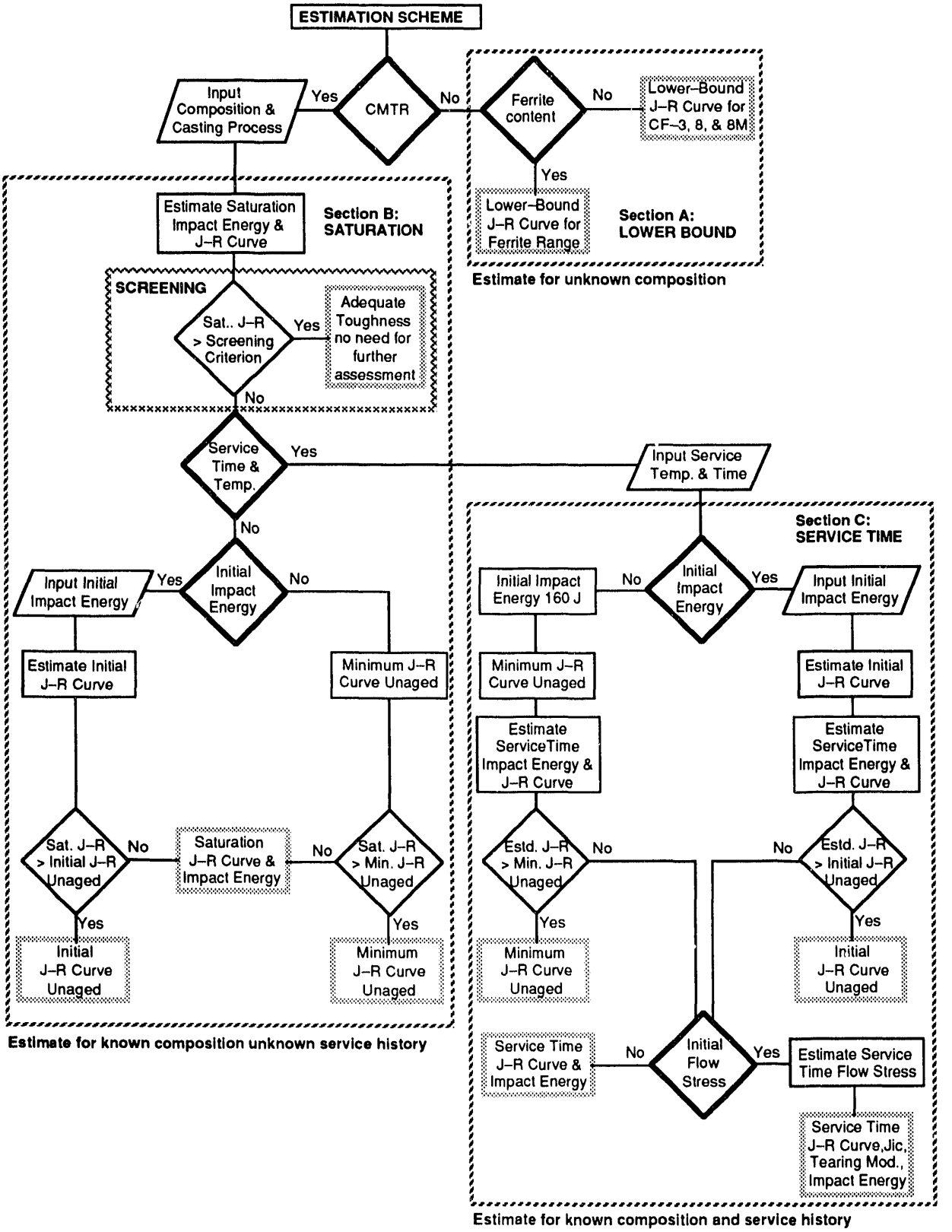

Figure 3. Flow diagram for estimating mechanical properties of aged cast stainless steels in LWR systems

material. It is possible that the estimations of saturation fracture toughness based on chemical composition are higher than the fracture toughness of the unaged material. Some cast stainless steels are inherently weak and may have poor fracture properties in the unaged condition. When information is available on the initial fracture toughness or initial RT Charpy-impact energy for estimating fracture toughness of a material, and when the J-R curve estimated from the chemical composition is higher than the initial fracture toughness of unaged material, the latter is used as the saturation J-R curve of the material. Such cast stainless steels are relatively insensitive to thermal aging and the fracture toughness of the material would not change during reactor service. Furthermore, when no information is available on the initial fracture toughness of a material, the minimum fracture toughness of unaged cast stainless steels is used as an upper bound for the estimated fracture toughness, i.e., when the J-R curve estimated from the chemical composition is higher than the minimum fracture toughness of unaged cast stainless steels, the latter is used as the saturation J-R curve of a material.

Estimation of mechanical properties at any given time and temperature of service, i.e., service time properties, is described in Section C. The initial impact energy and flow stress of the unaged material are required for these estimations. If not known, the initial impact energy can be assumed to be 200 J/cm^2. However, similar to Section B, initial fracture toughness of the unaged material or the minimum fracture toughness of unaged cast stainless steels is used as a upper bound for the estimations. The J_{IC} value and tearing modulus are determined from the estimated J-R curve and flow stress.

3.1 Estimate for Steels of Unknown Composition – Lower Bound Values

For cast stainless steels of unknown chemical composition within ASTM Specification A 351, lower-bound fracture toughness is defined for a given material grade and temperature. The cast stainless steels used in the U.S. nuclear industry generally contain <15% ferrite. The lower-bound fracture properties for a specific grade of steel are based on the "worst case" chemical composition and are thus very conservative for most steels. More realistic estimates of lower-bound properties are obtained if the ferrite content of the steel is known. The values of the coefficient C and exponent n of the power-law J-R curve, representing the lower-bound J-R curve for aged cast stainless steels with <10%, 10-15%, and >15% ferrite, are given in Table 1. The lower-bound J-R curves at RT and 290°C for static- and centrifugally cast CF-3, CF-8, and CF-8M steels are shown in Figs. 4 and 5.

3.2 Estimate for Steels of Known Composition and Unknown Service History – Saturation Values

When a CMTR is available, the saturation RT impact energy of a specific cast stainless steel is determined from the chemical composition and ferrite content of the material. The ferrite content is calculated from chemical composition in terms of the Hull's equivalent factors[31]

$$Cr_{eq} = Cr + 1.21(Mo) + 0.48(Si) - 4.99 \quad (1)$$

and

$$Ni_{eq} = (Ni) + 0.11(Mn) - 0.0086(Mn)^2 + 18.4(N) + 24.5(C) + 2.77. \quad (2)$$

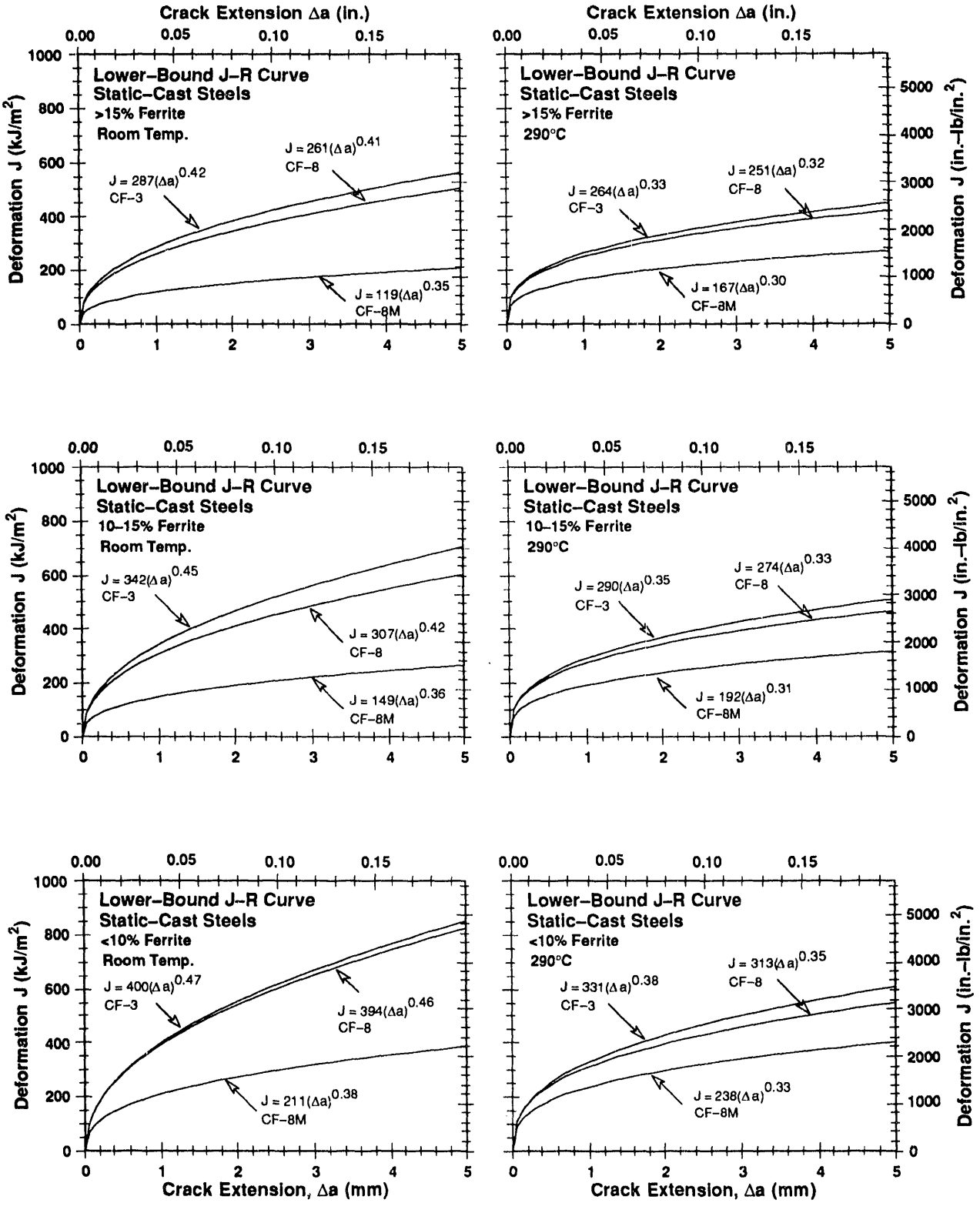

Figure 4. Lower-bound J-R curves at RT and 290°C for static-cast stainless steels with ferrite contents >15, 10–15, or <10%

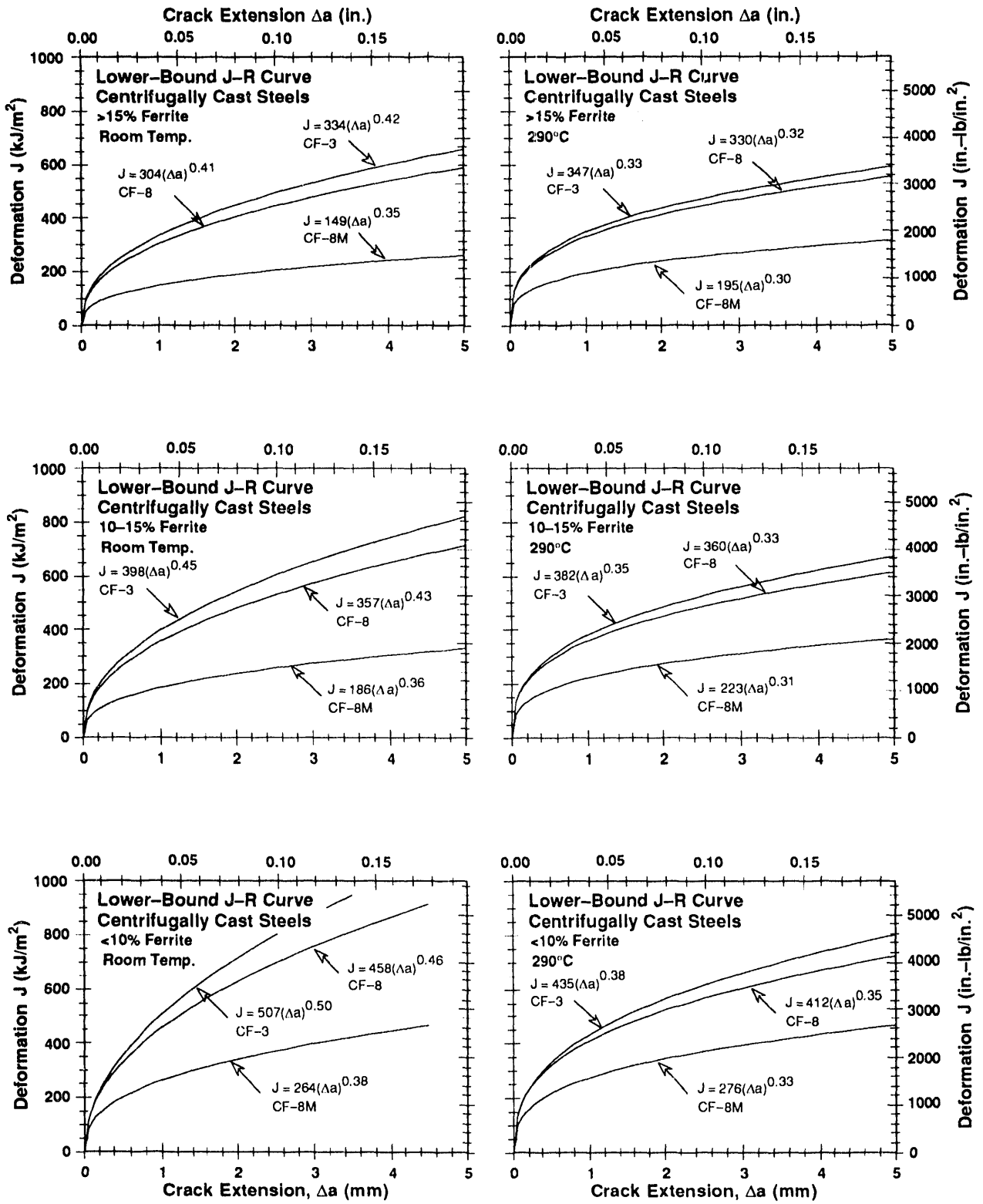

Figure 5. Lower-bound J-R curves at RT and 290°C for centrifugally cast stainless steels with ferrite contents >15, 10–15, or <10%

Table 1. Values of the coefficient C and exponent n for the lower bound J-R curve for cast stainless steels

Ferrite Content (%)	Grade	C_V (J/cm^2)	Static-Cast				Centrifugally Cast			
			Room Temp.		290°C		Room Temp.		290°C	
			C	n	C	n	C	n	C	n
>15	CF-3	30	287	0.42	264	0.33	334	0.42	347	0.33
	CF-8	25	261	0.41	251	0.32	304	0.41	330	0.32
	CF-8M	20	119	0.35	167	0.30	149	0.35	195	0.30
10-15	CF-3	42	342	0.45	290	0.35	398	0.45	382	0.35
	CF-8	34	307	0.42	274	0.33	357	0.43	360	0.33
	CF-8M	28	149	0.36	192	0.31	186	0.36	223	0.31
<10	CF-3	67	400	0.47	331	0.38	507	0.50	435	0.38
	CF-8	55	394	0.46	313	0.35	458	0.46	412	0.35
	CF-8M	47	211	0.38	238	0.33	264	0.38	276	0.33

The concentration of N is often not available in the CMTR; if not known, it is assumed to be 0.04 wt.%. The ferrite content δ_c is given by

$$\delta_c = 100.3(Cr_{eq}/Ni_{eq})^2 - 170.72(Cr_{eq}/Ni_{eq}) + 74.22. \quad (3)$$

The measured and calculated values of ferrite content for the various heats used in studies at ANL,[4] GF,[15] Electricité de France (EdF),[17] National Power (NP),[18] FRA,[19] and EPRI[21] are shown in Fig. 6. For most heats, the difference between the estimated and measured values is ±6% ferrite. The few heats for which the calculated ferrite content is significantly lower than the measured values generally contain ≥10% nickel.

Two different approaches are used to estimate the saturation RT Charpy-impact energy of the various grades of cast stainless steel. The saturation RT impact energy C_{Vsat} is expressed in terms of a material parameter Φ as follows:

$$\log_{10}C_{Vsat} = a + b\exp(-c\Phi), \quad (4)$$

where the values of the constants a, b, and c for different grades of steel are given in Table 2. For CF-3 and CF-8 steels, the material parameter Φ is expressed as

$$\Phi = \delta_c(Cr + Si)(C + 0.4N), \quad (5)$$

and for the Mo-bearing CF-8M steels as

Table 2. Values of the constants in Eq. 4 for estimating saturation RT Charpy-impact energy for cast stainless steels

Grade	Constants in Eq. 4		
	a	b	c
CF-3, CF-8	1.15	1.36	-0.035
CF-8M (<10% Ni)	1.10	2.12	-0.041
CF-8M (>10% Ni)	1.10	2.64	-0.064

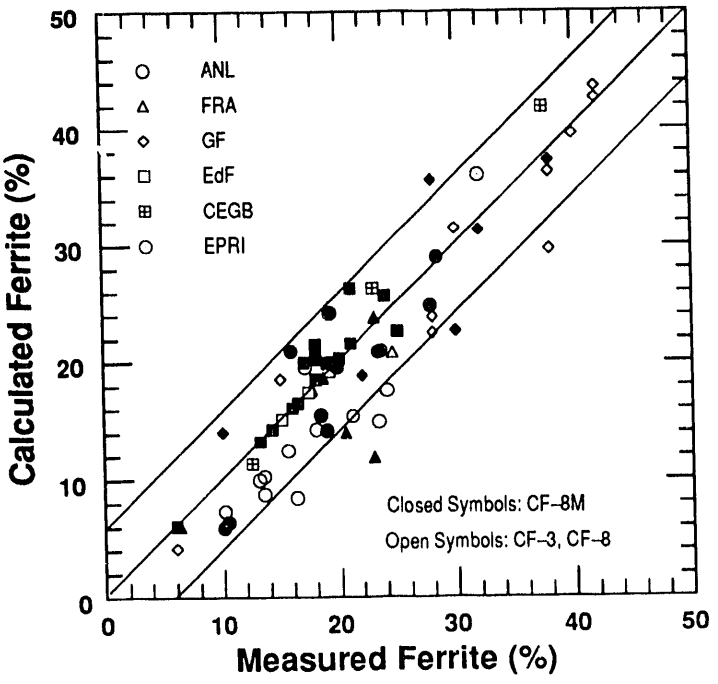

Figure 6. Measured and calculated ferrite content of various heats of cast stainless steel. The band represents ±6% deviation.

$$\Phi = \delta_c(Ni + Si + Mn)^2(C + 0.4N)/5. \quad (6)$$

The N content in Eqs. 5 and 6 can be assumed to be 0.04 wt.% if the value is not known. Figure 7 shows the saturation values of RT impact energy for CF-3, CF-8, and CF-8M steels predicted by Eqs. 4-6 and those observed experimentally at ANL,[4-6] GF,[15] Westinghouse (WH),[16] EdF,[17] NP,[18] FRA,[19] and EPRI.[21] The chemical composition, ferrite content, and saturation RT Charpy-impact energy of the materials from ANL, GF, FRA, WH, and EPRI studies are given in Table 3. The difference between the predicted and observed values is $\leq \pm 15\%$ for most of the CF-3 and CF-8 steels and $\leq \pm 25\%$ for the CF-8M steels.

In the second approach, saturation RT impact energy C_{Vsat} is estimated directly from the chemical composition of the steel, without the ϕ parameter. For CF-3 and CF-8 steels, C_{Vsat} is given by

$$\log_{10}C_{Vsat} = 5.64 - 0.006\delta_c - 0.185Cr + 0.273Mo - 0.204Si + 0.044Ni - 2.12(C + 0.4N), \quad (7)$$

and for CF-8M steels by

$$\log_{10}C_{Vsat} = 7.28 - 0.011\delta_c - 0.185Cr - 0.369Mo - 0.451Si - 0.007Ni - 4.71(C + 0.4N). \quad (8)$$

Table 3. Chemical composition, ferrite content, and kinetics of thermal embrittlement for various heats of cast stainless steels

	Chemical Composition (wt.%)							Ferrite (%)		C_{Vsat}	Constants			Q
Heat	Cr	Mo	Si	Ni	Mn	C	N	Calc.	Meas.	(J/cm^2)	β	θ	α	(kJ/mole)
Argonne														
52	19.49	0.35	0.92	9.40	0.57	0.009	0.052	10.3	13.5	161.8	–	–	–	–
51	20.13	0.32	0.86	9.06	0.63	0.010	0.058	14.3	18.0	115.9	0.139	3.53	1.15	204.7
47	19.81	0.59	1.06	10.63	0.60	0.018	0.028	8.4	16.3	163.7	0.069	2.29	1.20	195.7
P2	20.20	0.16	0.94	9.38	0.74	0.019	0.040	12.5	15.6	141.3	0.258	2.83	1.09	218.6
I	20.20	0.45	0.83	8.70	0.47	0.019	0.032	20.4	17.1	134.3	0.094	2.10	1.00	250.0
69	20.18	0.34	1.13	8.59	0.63	0.023	0.028	21.0	23.6	76.7	0.214	3.21	1.07	175.9
P1	20.49	0.04	1.12	8.10	0.59	0.036	0.057	17.6	24.1	53.7	0.305	2.57	0.75	252.7
61	20.65	0.32	1.01	8.86	0.65	0.054	0.080	10.0	13.1	93.3	0.214	3.48	1.20	197.8
59	20.33	0.32	1.08	9.34	0.60	0.062	0.045	8.8	13.5	89.1	0.197	3.14	1.20	249.4
68	20.64	0.31	1.07	8.08	0.64	0.063	0.062	14.9	23.4	47.1	0.301	2.88	0.68	161.1
60	21.05	0.31	0.95	8.34	0.67	0.064	0.058	15.4	21.1	44.8	0.291	2.89	0.88	210.9
56	19.65	0.34	1.05	9.28	0.57	0.066	0.030	7.3	10.1	117.6	–	–	–	–
74	19.11	2.51	0.73	9.03	0.54	0.064	0.048	15.5	18.4	63.1	0.269	3.44	0.70	95.0
75	20.86	2.58	0.67	9.12	0.53	0.065	0.052	24.8	27.8	32.1	0.436	2.82	0.51	139.0
66	19.45	2.39	0.49	9.28	0.60	0.047	0.029	19.6	19.8	87.9	0.208	3.16	1.57	163.9
64	20.76	2.46	0.63	9.40	0.60	0.038	0.038	29.0	28.4	41.1	0.338	2.81	0.60	147.3
65	20.78	2.57	0.48	9.63	0.50	0.049	0.064	20.9	23.4	59.7	0.260	2.99	0.59	153.8
P4	19.64	2.05	1.02	10.00	1.07	0.040	0.151	5.9	10.0	62.7	0.289	2.70	0.62	158.7
63	19.37	2.57	0.58	11.85	0.61	0.055	0.031	6.4	10.4	126.5	0.119	2.83	1.11	155.5
Georg Fischer Co.														
284	23.00	0.17	0.52	8.23	0.28	0.025	0.037	43.6	42.0	20.5	0.551	3.66	0.39	85.9
280	21.60	0.25	1.37	8.00	0.50	0.028	0.038	36.3	38.0	19.6	0.609	3.20	0.73	88.9
282	22.50	0.15	0.35	8.53	0.43	0.035	0.040	29.7	38.0	28.5	0.500	3.65	0.39	91.6
281	23.10	0.17	0.45	8.60	0.41	0.036	0.053	31.4	30.0	17.2	0.618	3.76	0.47	89.8
283	22.60	0.23	0.53	7.88	0.48	0.036	0.032	42.6	42.0	18.6	0.599	3.60	0.44	83.7
278	20.20	0.13	1.00	8.27	0.28	0.038	0.030	18.5	15.0	68.3	0.347	3.90	0.29	63.1
279	22.00	0.22	1.36	7.85	0.37	0.040	0.032	39.5	40.0	23.8	0.546	3.06	0.58	93.5
277	20.50	0.06	1.81	8.13	0.54	0.052	0.019	22.5	28.0	30.7	0.466	3.54	0.49	87.7
291	19.60	0.66	1.59	10.60	0.28	0.065	0.054	4.2	6.0	121.9	0.195	3.65	0.35	71.2
292	21.60	0.13	1.57	7.52	0.34	0.090	0.039	23.9	28.0	17.2	0.373	3.07	0.44	98.8
290	20.00	2.40	1.51	8.30	0.41	0.054	0.050	31.3	32.0	15.8	0.624	3.48	0.12	81.0
288	19.60	2.53	1.70	8.40	0.47	0.052	0.022	35.6	28.0	14.9	0.671	2.96	0.66	105.3
287	20.50	2.58	0.51	8.46	0.50	0.047	0.033	37.2	38.0	20.5	0.555	3.46	0.36	90.3
286	20.20	2.44	1.33	9.13	0.40	0.072	0.062	18.9	22.0	15.5	0.594	3.03	0.72	106.4
289	19.70	2.30	1.44	8.25	0.48	0.091	0.032	22.6	30.0	16.2	0.580	3.29	0.41	90.1
285	18.80	2.35	0.86	9.49	0.48	0.047	0.039	14.0	10.0	61.1	0.313	3.60	0.20	89.3
Framatome														
A	18.90	0.10	0.99	8.90	1.14	0.021	0.074	6.0	6.3	166.0	0.090	3.44	0.20	111.7
E	21.04	0.08	0.54	8.47	0.80	0.035	0.051	17.6	16.5	45.7	0.334	2.63	0.65	132.9
F	19.72	0.34	1.16	8.33	0.26	0.038	0.026	17.7	12.0	83.2	0.282	2.45	1.23	176.2
C	20.73	0.13	1.09	8.19	0.91	0.042	0.035	20.9	20.1	51.1	0.393	3.30	0.45	83.1
G	20.65	0.02	1.03	8.08	0.74	0.040	0.073	15.3	17.0	62.5	–	–	–	–
H	20.70	0.05	1.18	8.07	0.71	0.050	0.045	18.3	21.5	50.6	–	–	–	–
D	19.15	2.50	0.94	10.32	1.12	0.026	0.063	12.2	13.9	33.0	0.439	3.30	0.40	89.7
I	19.36	2.40	0.98	10.69	0.70	0.020	0.039	14.1	15.5	150.7	–	–	–	–
K	20.80	2.62	0.75	10.45	1.09	0.060	0.056	15.4	14.0	48.5	–	–	–	–
L	20.76	2.48	0.81	10.56	0.79	0.040	0.042	18.6	19.0	30.4	–	3.00	–	–
B	20.12	2.52	0.93	10.56	0.83	0.053	0.042	14.0	17.3	28.2	0.478	2.55	0.47	128.6
Westinghouse														
C1488	20.95	2.63	0.53	9.48	1.02	0.061	0.056	22.1	14.0	53.1	–	2.80	–	–
Electric Power Research Institute														
EPRI	22.04	0.23	0.84	7.93	0.74	0.030	0.045	36.0	32.0	30.0	0.564	2.10	0.60	225.0

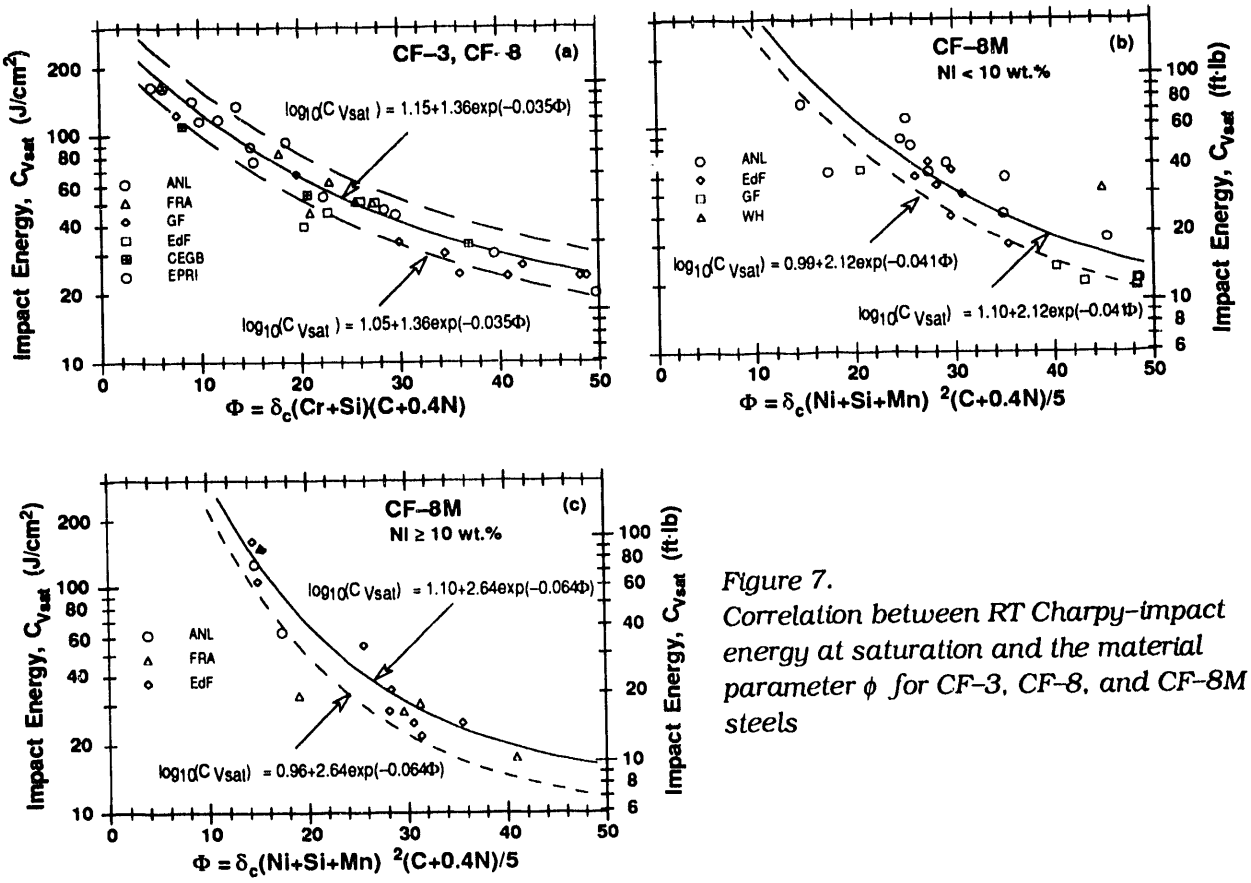

Figure 7.
Correlation between RT Charpy-impact energy at saturation and the material parameter ϕ for CF-3, CF-8, and CF-8M steels

To ensure that the estimates are either accurate or conservative for all heats, the saturation RT impact energy for a specific cast stainless steel should be determined by both of the methods given in Eqs. 4–8, and the lower value should be used for estimating fracture properties.

The saturation fracture toughness J-R curve for a specific cast stainless steel can be estimated from its RT impact energy at saturation. The J-R curve is expressed by the power-law relation $J_d = C\Delta a^n$. The coefficient C at RT or at reactor temperatures and the RT Charpy-impact energy for aged and unaged cast stainless steels are plotted in Fig. 8. Fracture toughness data from studies at ANL,[4-7] FRA,[19,20] EPRI,[21] The Welding Institute (TWI),[22] and Materials Engineering Associates, Inc. (MEA)[32] are included in the figure. At both RT and reactor temperatures, the coefficient C decreased with a decrease in impact energy. Separate correlations were obtained for CF-3 or CF-8 steels and for CF-8M steels; the latter showed a larger decrease in fracture toughness for a given impact energy. The correlations used to estimate J-R curves for static-cast materials were obtained by subtracting the value of σ (standard deviation for the fit to the data) from the best-fit curve; they are shown as dashed lines in Fig. 8, and help ensure that the estimated J-R curve is conservative for all material and aging conditions. Best-fit correlations were used for centrifugally cast materials. The saturation fracture toughness J-R curve for static- and centrifugally cast steels is given by

$$J_d = a[C_{Vsat}]^b[\Delta a]^n, \tag{9}$$

where the exponent n is defined as

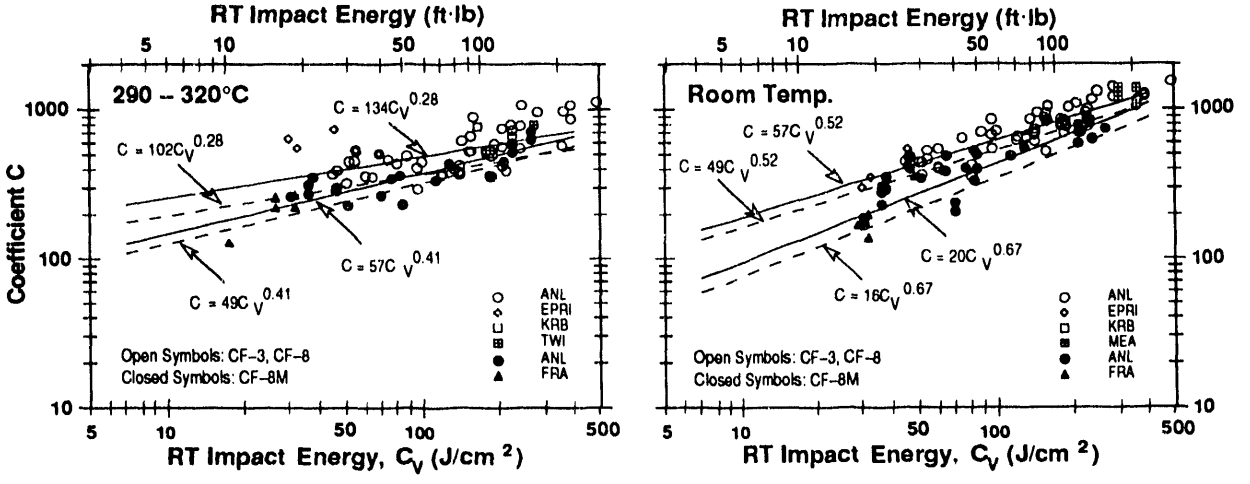

Figure 8. Correlation between RT Charpy-impact energy and coefficient C for cast stainless steel at 290–320°C and at RT. The solid and dashed lines represent the correlations used to estimate the J-R curves for centrifugally and static-cast materials, respectively.

$$n = c + d[\log_{10} C_{Vsat}], \tag{10}$$

and the values of constants a, b, c, and d for different grades of steel and test temperature are given in Tables 4 and 5. The J-R curve at any intermediate temperature can be linearly interpolated from the estimated values of C and n at RT and 290°C.

The fracture toughness J-R curve at saturation for a specific cast stainless steel can be obtained from its chemical composition by using the correlations for C_{Vsat} given in Eqs. 1–8 and then using the estimated C_{Vsat} in Eqs. 9 and 10 to obtain the J-R curve. Comparisons of

Table 4. Values of the constants in Eq. 9 for estimating the power-law J-R curve for cast stainless steels

	Static-Cast				Centrifugally Cast			
	Room Temp.		290°C		Room Temp.		290°C	
Grade	a	b	a	b	a	b	a	b
CF-3, CF-8	49	0.52	102	0.28	57	0.52	134	0.28
CF-8M	16	0.67	49	0.41	20	0.67	57	0.41

Table 5. Values of the constants in Eq. 10 for estimating exponent n of the power-law J-R curve for cast stainless steels

	Room Temp.		290–320°C	
Grade	c	d	c	d
CF-3	0.08	0.228	0.14	0.130
CF-8	0.22	0.139	0.22	0.074
CF-8M	0.25	0.077	0.23	0.057

the experimental and estimated J–R curves at saturation, i.e., the minimum fracture toughness that would be achieved for the material by thermal aging, are shown in Figs. 9–12. For most heats, the saturation fracture toughness is achieved after aging for 5000 h or more at 400°C (752°F). For comparison, the experimental and estimated J–R curves for the unaged materials are also shown in Fig. 9; the J–R curves were estimated from Eqs. 20–24 by using the measured initial RT impact energy $C_{V_{int}}$. The estimated J–R curves show good agreement with the experimental results in most cases and are essentially conservative. The largest difference between the estimated and experimental J–R curves is for centrifugally cast Heats P2 and 205 at RT and for centrifugally cast Heat P2 and the static-cast EPRI heat at 290°C; the estimated curves of these heats are 30–50% lower than those obtained experimentally. The experimental J–R curves for Heat 75, aged for 30,000 h at 350°C, are lower than those for 10,000–h aging at 400°C (shown in Fig. 11) and are in good agreement with the estimated saturation J–R curve.

Room-temperature J–R curves for unaged static-cast Heats 68, 69, and 75 are non-conservative. It is believed that the poor fracture toughness of these unaged static-cast slabs is due to residual stresses introduced into the material during the casting process or production heat treatment. Annealing these heats for a short time at temperatures between 290 and 400°C (554 and 752°F) increased the fracture toughness and decreased the tensile stress without significantly affecting the impact energy;[6,7] consequently, the fracture toughness of these heats would initially increase during reactor service before it would decrease as a result of thermal aging.

The estimated J–R curve after 32 efpy of service at 320°C (608°F) is also shown in Figs. 9–12. The results indicate that, at 320°C service, fracture toughness of these materials will reach saturation or will be close to saturation within the 40–yr design life.

A screening criterion is used with the saturation fracture properties to determine whether a detailed assessment of thermal embrittlement is required for the material. Cast stainless steel components with adequate saturation fracture toughness or impact energy would not require any further evaluation of thermal embrittlement. For screening purposes, an elastic-plastic fracture toughness, J_d, value of 525 kJ/m^2 (determined for a crack extension of 10 mm and at reactor temperatures) may be considered to provide more than adequate structural integrity for the components of interest. A lower value may also be used, depending on the particular component.

The correlations described in Eqs. 4–10 account for the degradation of mechanical properties and do not consider the initial fracture properties of the unaged material. When no information is available on the initial fracture toughness of a specific material, the minimum fracture toughness of unaged cast stainless steels is used as the upper bound for the predicted fracture toughness of the aged material. The available fracture toughness J–R curve data at 290–320°C (555–610°F) for unaged cast stainless steels are shown in Fig. 13a. The static-cast pump casing ring (Heat C1 with δ_c = 8%) shows the lowest and the centrifugally cast pipes (Heat P2 with δ_c = 12% and Heat C1488 with δ_c = 21%) exhibit the highest fracture toughness. Fracture toughness J–R curves for wrought stainless steels are higher than the J–R curve for the static-cast pump casing ring; see Fig. 13b. The fracture toughness of unaged cast stainless steels is slightly higher at RT than at 290–320°C. At temperatures between RT and 320°C, the minimum fracture toughness of unaged static-cast stainless steels can be expressed as

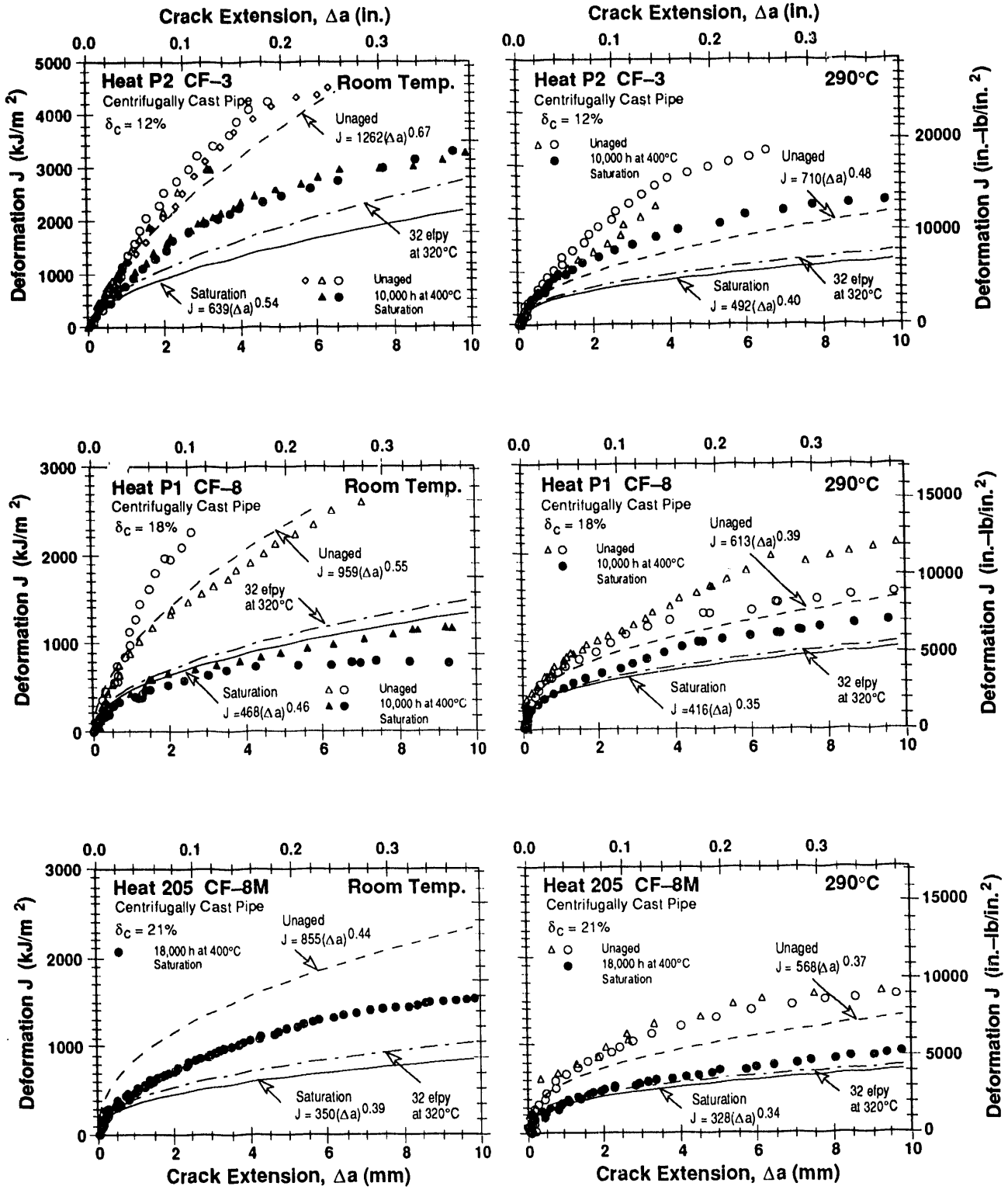

Figure 9. Saturation fracture toughness J-R curves at RT and 290°C estimated from the chemical composition of centrifugally cast CF-3, CF-8, and CF-8M pipes, and determined experimentally

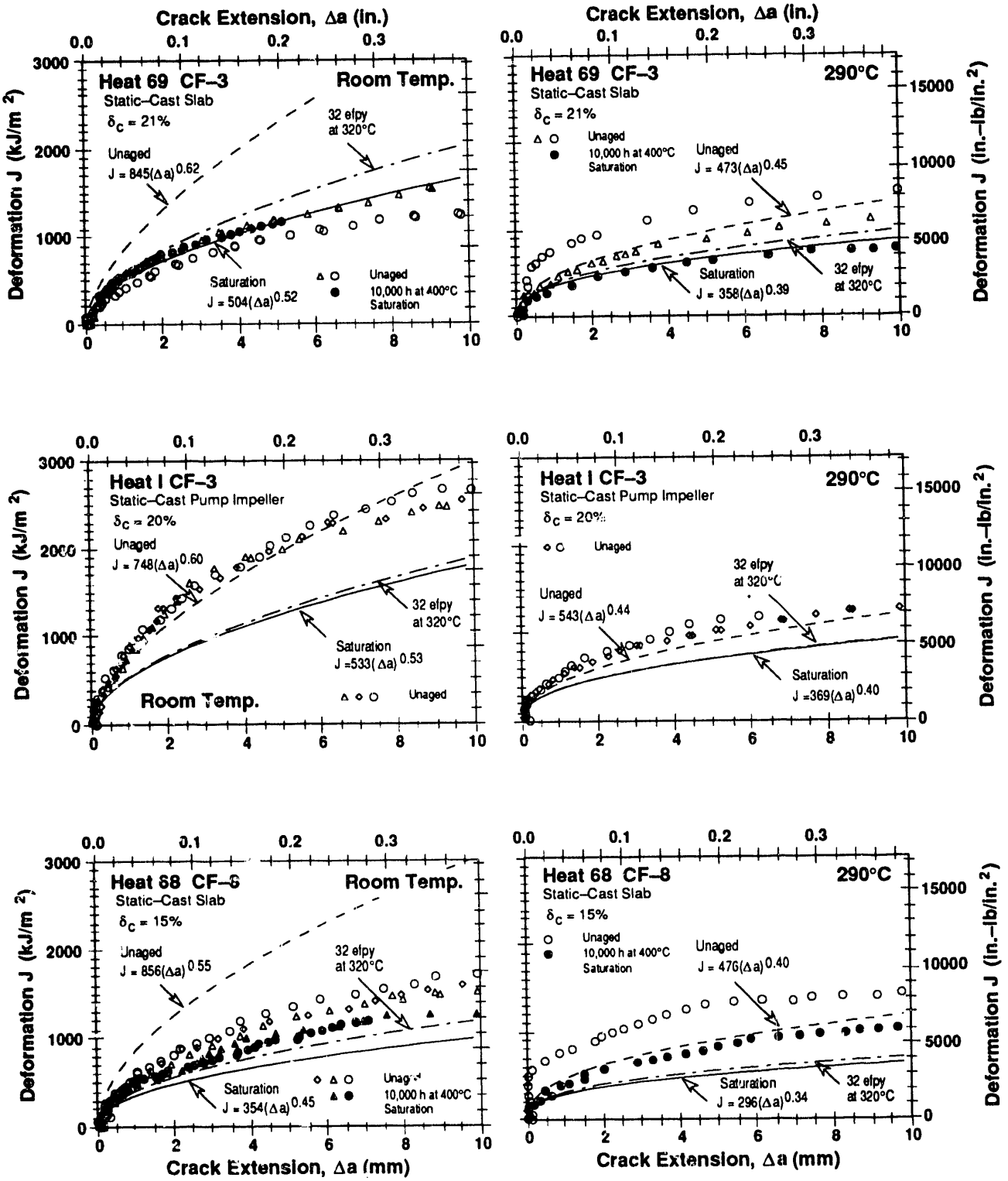

Figure 10. Saturation fracture toughness J-R curves at RT and 290°C estimated from the chemical composition of static-cast CF-3 and CF-8 steels, and determined experimentally

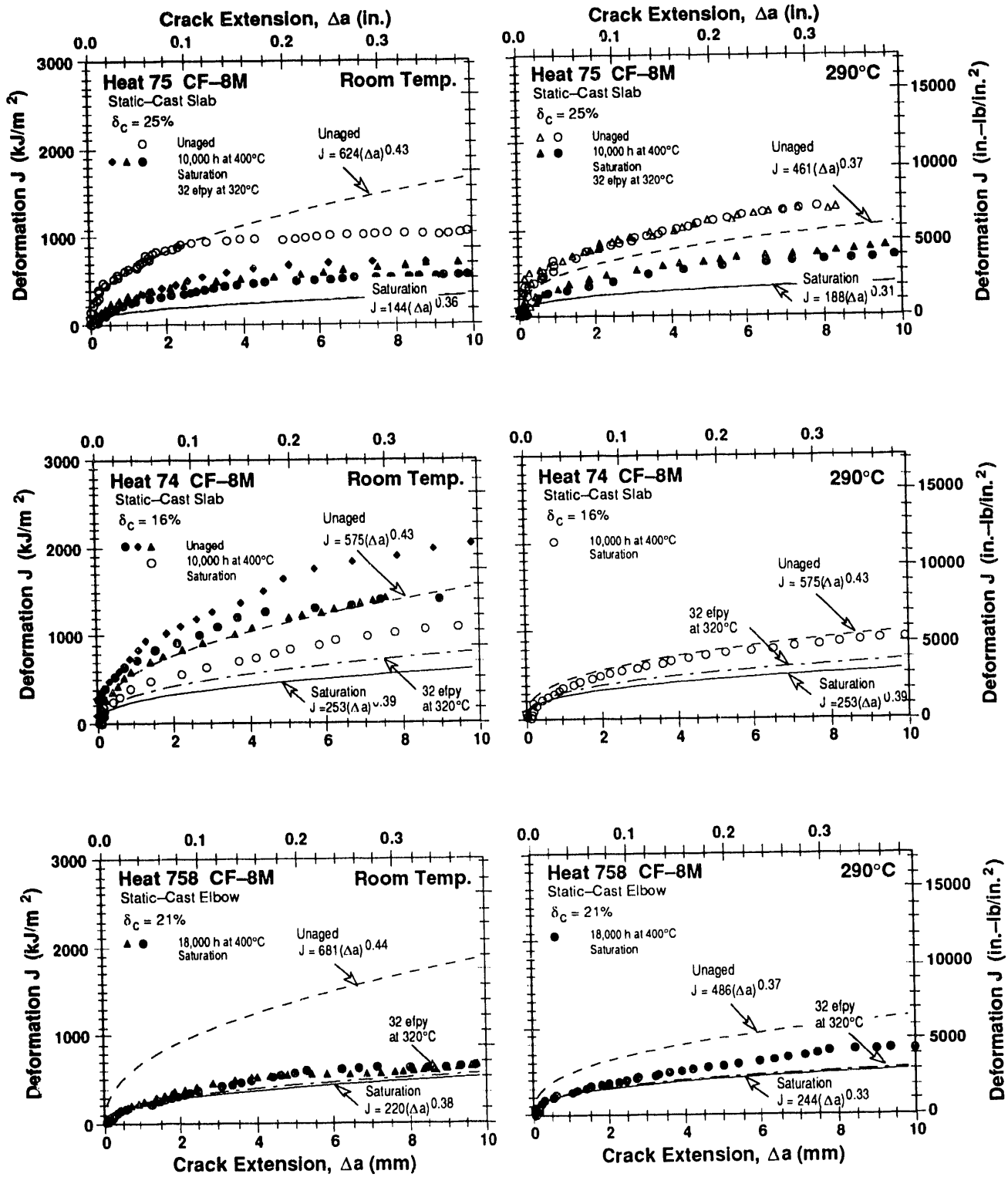

Figure 11. Saturation fracture toughness J-R curves at RT and 290°C estimated from the chemical composition of static-cast CF-8M steels, and determined experimentally

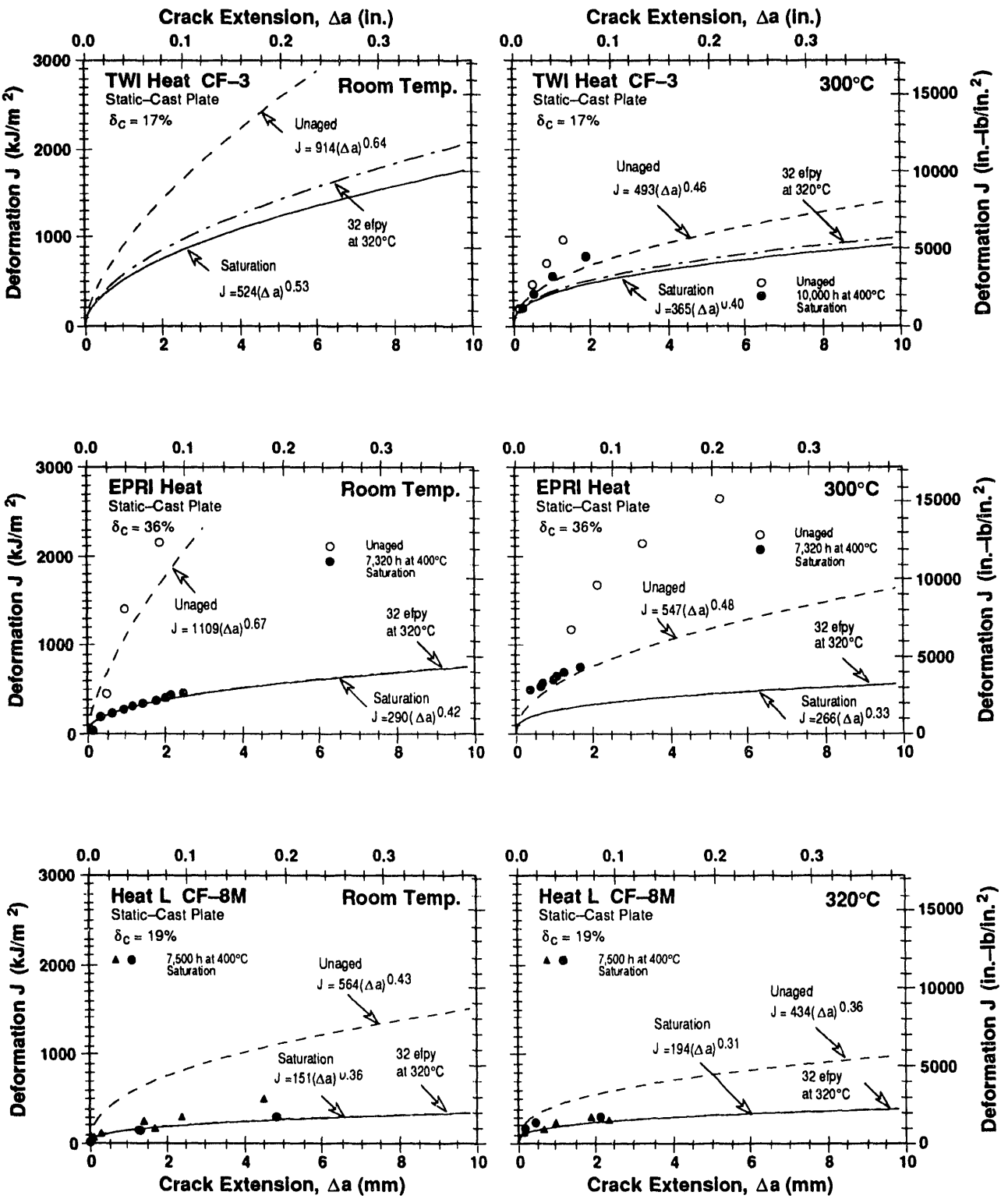

Figure 12. Saturation fracture toughness J-R curves at RT and 290°C estimated from the chemical composition of static-cast CF-3 and CF-8M steels, and determined experimentally (Refs. 19,21,22)

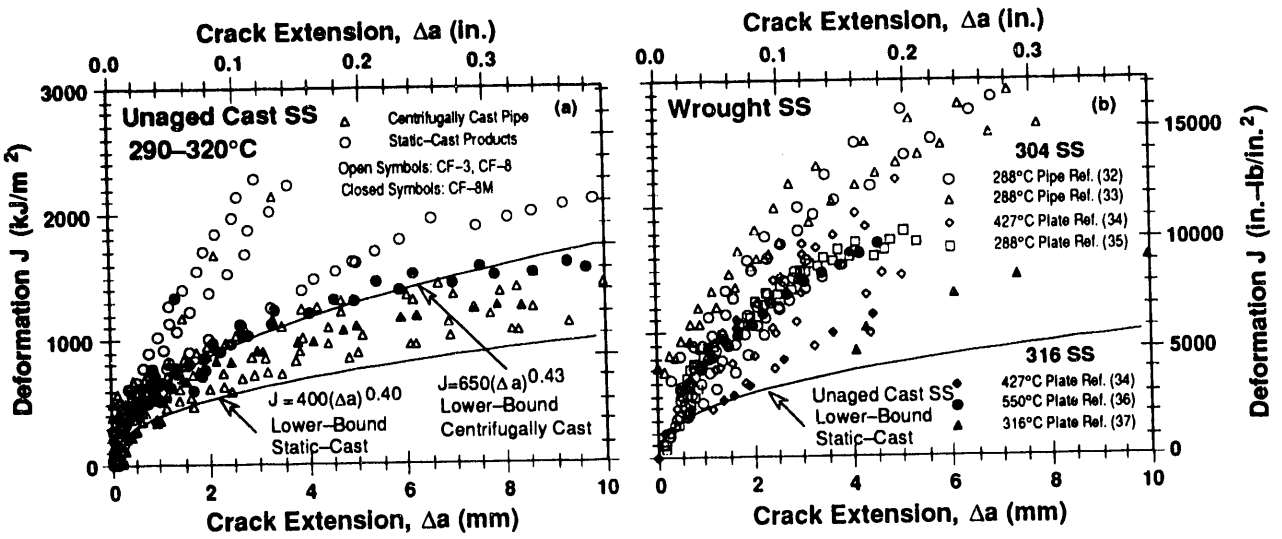

Figure 13. Fracture toughness J-R curve for (a) unaged cast stainless steels and (b) wrought stainless steels at temperatures ≥290°C

$$J_d = 400[\Delta a]^{0.40} \tag{11}$$

and of centrifugally cast stainless steels as

$$J_d = 650[\Delta a]^{0.43}. \tag{12}$$

When the J-R curve estimated from the chemical composition is higher than the minimum fracture toughness of unaged cast stainless steels, the latter is used as the saturation J-R curve of a material. Initial fracture toughness of the unaged material is required to justify the use of estimated J-R curves higher than those given by Eq. 11 or 12.

The CMTR for a specific cast stainless steel component provides information on chemical composition, tensile strength, and possibly Charpy-impact energy of the material; fracture toughness is not available in CMTRs. The fracture toughness J-R curve for unaged material may be obtained by using the initial RT Charpy-impact energy, C_{Vint}, instead of C_{Vsat} in Eqs. 9 and 10. When the initial fracture toughness or initial RT Charpy-impact energy for estimating fracture toughness of a material is known, and when the J-R curve estimated from the chemical composition is higher than the initial fracture toughness of unaged material, the latter is used as the saturation J-R curve of the material. Such cases represent low fracture toughness materials that are relatively insensitive to thermal aging; thus, fracture toughness of the material would not change during reactor service.

3.3 Estimate for Steels of Known Composition and Service History – Service Time Values

Room-temperature impact energy as a function of time and temperature of aging is estimated from the RT saturation impact energy C_{Vsat} and the kinetics of embrittlement. The decrease in RT Charpy-impact energy C_V with time is expressed as

$$\log_{10}C_V = \log_{10}C_{Vsat} + \beta\{1 - \tanh[(P - \theta)/\alpha]\} \tag{13}$$

where the aging parameter P is defined by

$$P = \log_{10}(t) - \frac{1000Q}{19.143}\left(\frac{1}{T_s+273} - \frac{1}{673}\right). \quad (14)$$

The constants α and β can be determined from C_{Vint} and C_{Vsat}, as follows

$$\alpha = -0.585 + 0.795\log_{10}C_{Vsat}. \quad (15)$$

and

$$\beta = (\log_{10}C_{Vint} - \log_{10}C_{Vsat})/2. \quad (16)$$

If C_{Vint} is not known, a typical value of 200 J/cm^2 may be used. The value of θ varies with service temperature; it is 3.3 for temperatures <280°C, 2.9 for temperatures of 280–330°C, and 2.5 for temperatures of 330–360°C. Activation energy for thermal embrittlement is expressed in terms of both chemical composition and the constant θ. The activation energy Q is given by

$$Q = 10\,[74.52 - 7.20\,\theta - 3.46\,Si - 1.78\,Cr - 4.35\,I_1\,Mn + (148 - 125\,I_1)\,N - 147\,I_2\,C], \quad (17)$$

where the indicators $I_1 = 0$ and $I_2 = 1$ for CF-3 or CF-8 steels and assume the values of 1 and 0, respectively, for CF-8M steels. Equation 17 is based on Charpy-impact data obtained from materials that were aged up to 58,000 h at 290–400°C and is an updated version of an expression presented earlier.[9] The estimated and observed values of Q for the ANL,[1-6] GF,[15] EdF,[17] NP,[18] and FRA[19] heats are plotted in Fig. 14. The predicted values are within the 95% confidence limits for all the heats. Equation 17 is applicable to compositions within ASTM Specification A 351, with an upper limit of 1.2 wt.% for Mn content. Actual Mn content is used when materials contain up to 1.2 wt.% Mn; for steels containing >1.2 wt.% Mn, 1.2 wt.% is assumed. Furthermore, the values of Q predicted from Eq. 17 should be between 65 kJ/mole

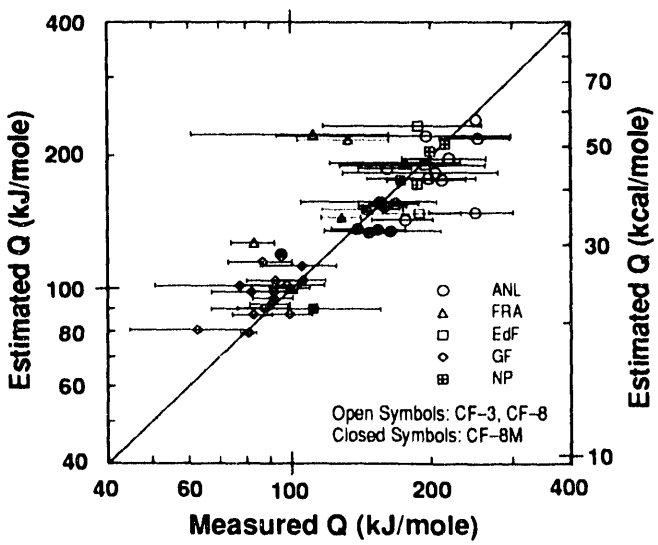

Figure 14. Observed and estimated activation energy for thermal embrittlement

minimum and 250 kJ/mole maximum; Q is assumed to be 65 kJ/mole if the predicted values are lower and 250 kJ/mole if the predicted values are higher.

The correlation expressed by Eq. 18 qualitatively agrees with the microstructural and mechanical-property data. For example, an increase in the value of θ decreases the activation energy, as expected. The contributions of Si for all grades of steel and Mn for CF-8M steels are consistent with their effect on G-phase precipitation. These elements should promote precipitation of G phase: hence, the coefficients for these elements should have a negative sign because activation energy for thermal embrittlement is low for steels that show G-phase precipitation. An increase in C or N in the steel will promote carbide or nitride precipitation at high temperatures and thus increase the activation energy. The positive sign of the coefficient for N agrees with this behavior. The coefficient of C in CF-8M steel, however, has a negative sign. It is likely that C also promotes precipitation of G phase, a multicomponent phase consisting of Ni, Si, Mo, Cr, Fe, and some Mn and C.[24,28]

The RT Charpy-impact energy of a specific cast stainless steel as a function of service time and temperature can be obtained from estimated C_{Vsat} (Eqs. 4–8) and the kinetics of embrittlement (Eqs. 13–17). The initial Charpy-impact energy of the unaged steel is needed for estimating the decrease in impact energy as a function of time and temperature of service. The fracture toughness J-R curve is then obtained by using the estimated RT Charpy-impact energy, C_V, in Eqs. 9 and 10. However, depending on the available information, minimum fracture toughness of cast stainless steels (Eqs. 11 or 12) or initial fracture toughness of the unaged material is used as an upper bound for the estimations.

The RT Charpy-impact energy observed experimentally and that estimated from the chemical composition and initial impact energy of the ANL,[4-7] GF,[15] EdF,[17] FRA,[19] and EPRI[21] heats aged at temperatures between 290 and 350°C (554 and 662°F) are shown in Figs. 15 and 16. The estimates for 31 of the 47 heats used in developing the correlations for the kinetics of thermal embrittlement of cast stainless steels are shown in these figures. A θ value of 2.9 was used for all temperatures of thermal aging. The estimated change in impact energy at temperatures ≤330°C (626°F) is either accurate or slightly conservative for most of the heats. A few heats show poor agreement because either the estimated C_{Vsat} is higher than the experimental value, e.g., FRA Heat D and ANL Heat 47, or the estimated activation energy is high, e.g., FRA Heat C and GF Heat 278. Even at 350°C, the estimated impact energies show good agreement with the experimental results because the θ values for most of the heats shown in the figures are either greater or only slightly lower than 2.9. The EPRI heat and EdF Heat A10 (experimental θ is 2.1 for both heats) alone show non-conservative estimates at 350°C. A θ value of 2.5 rather than 2.9 should be used to ensure that the estimates at 330—360°C (626–680°F) are conservative.

Examples of the experimental and estimated J-R curves for several partially aged (e.g., 30,000 h at 320°C) cast stainless steels are shown in Figs. 17 and 18. The estimated J-R curves show good agreement with experimental results.

Tensile flow stress of aged cast stainless steels can be estimated from correlations between the ratio of the tensile flow stress of aged and unaged cast stainless steels and a normalized aging parameter. The ratio of the tensile flow stress of aged and unaged cast stainless steels at RT and 290°C (554°F) is plotted as a function of a normalized aging parameter in Fig. 19. Flow stress is characterized as the mean of the 0.2% yield stress and ultimate stress, and the aging

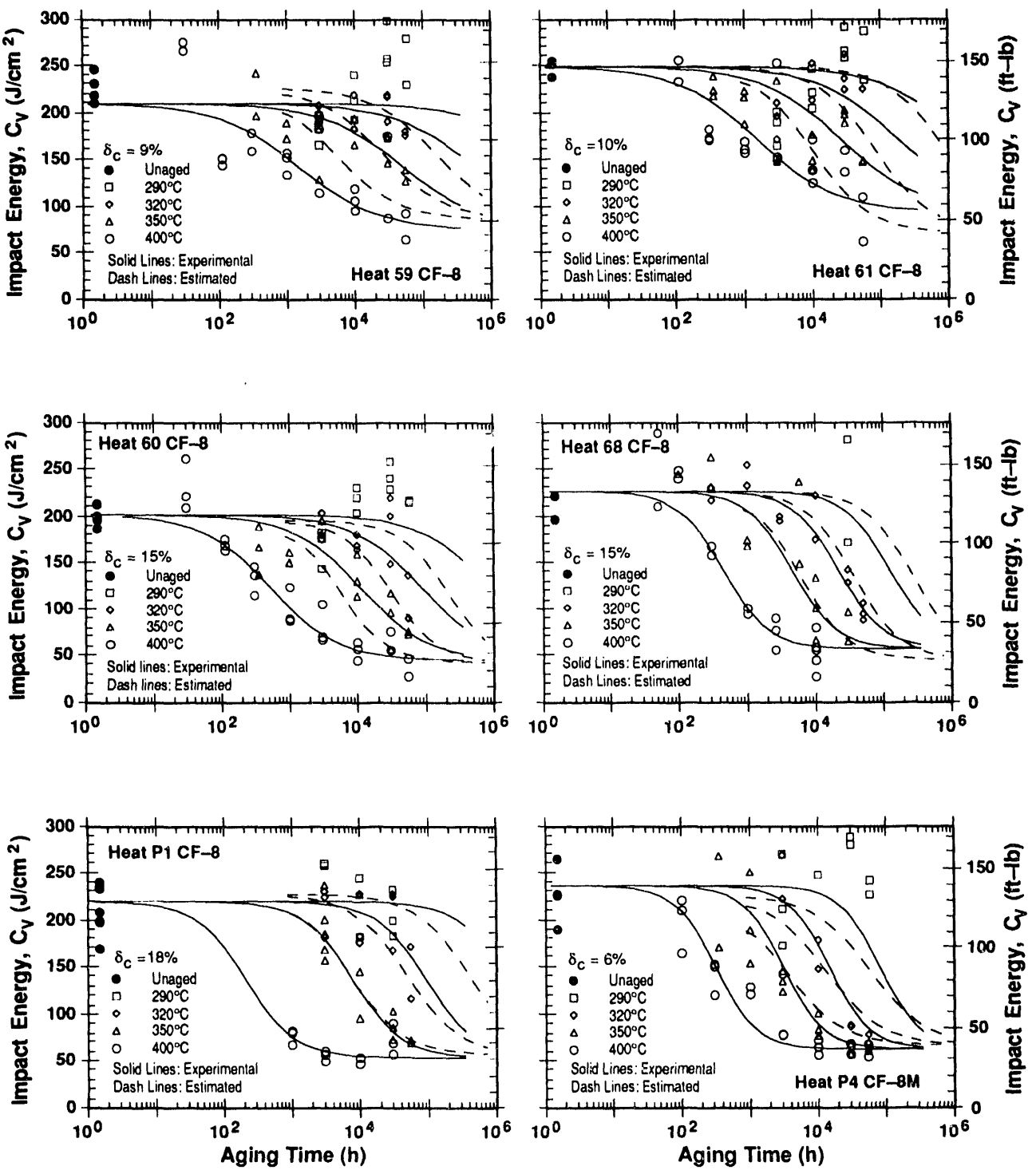

Figure 15. RT Charpy-impact energy for 16 ANL heats and 1 EPRI heat observed experimentally and estimated from the composition and initial impact energy of the materials. Solid lines represent the best fit of the data at 290–400°C and dash lines are the estimates at 290–350°C.

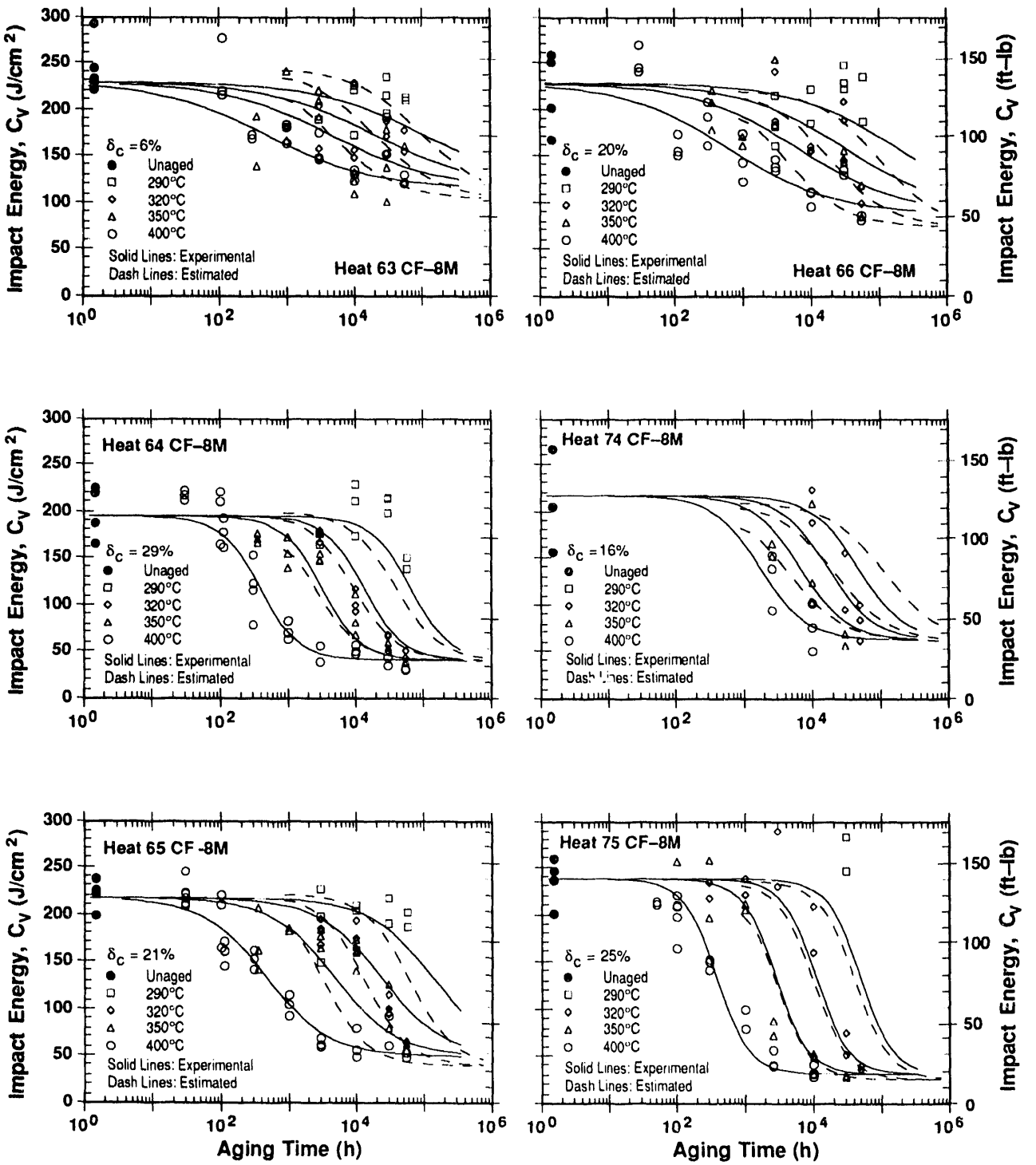

Figure 15. (Contd.)

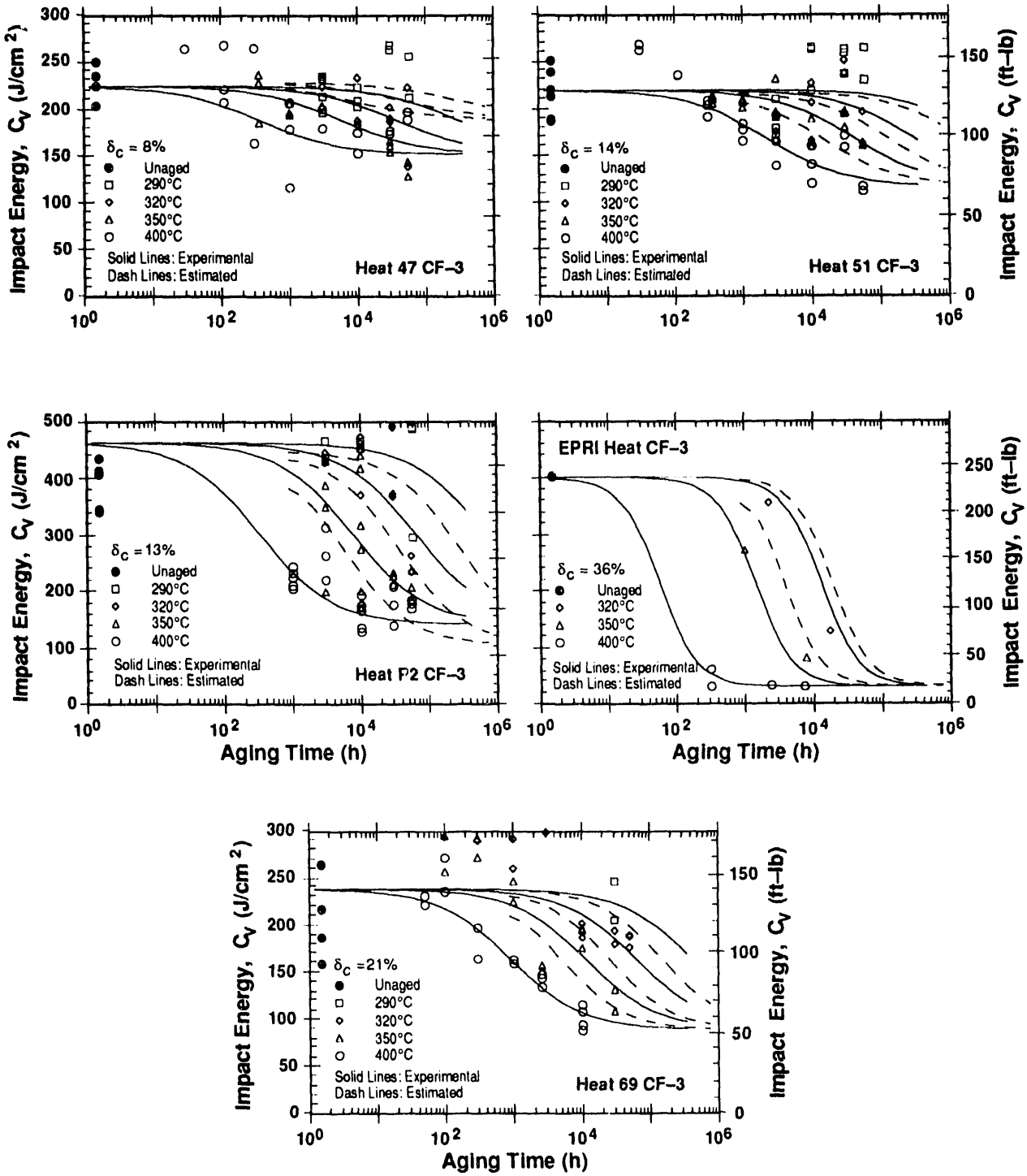

Figure 15. (Contd.)

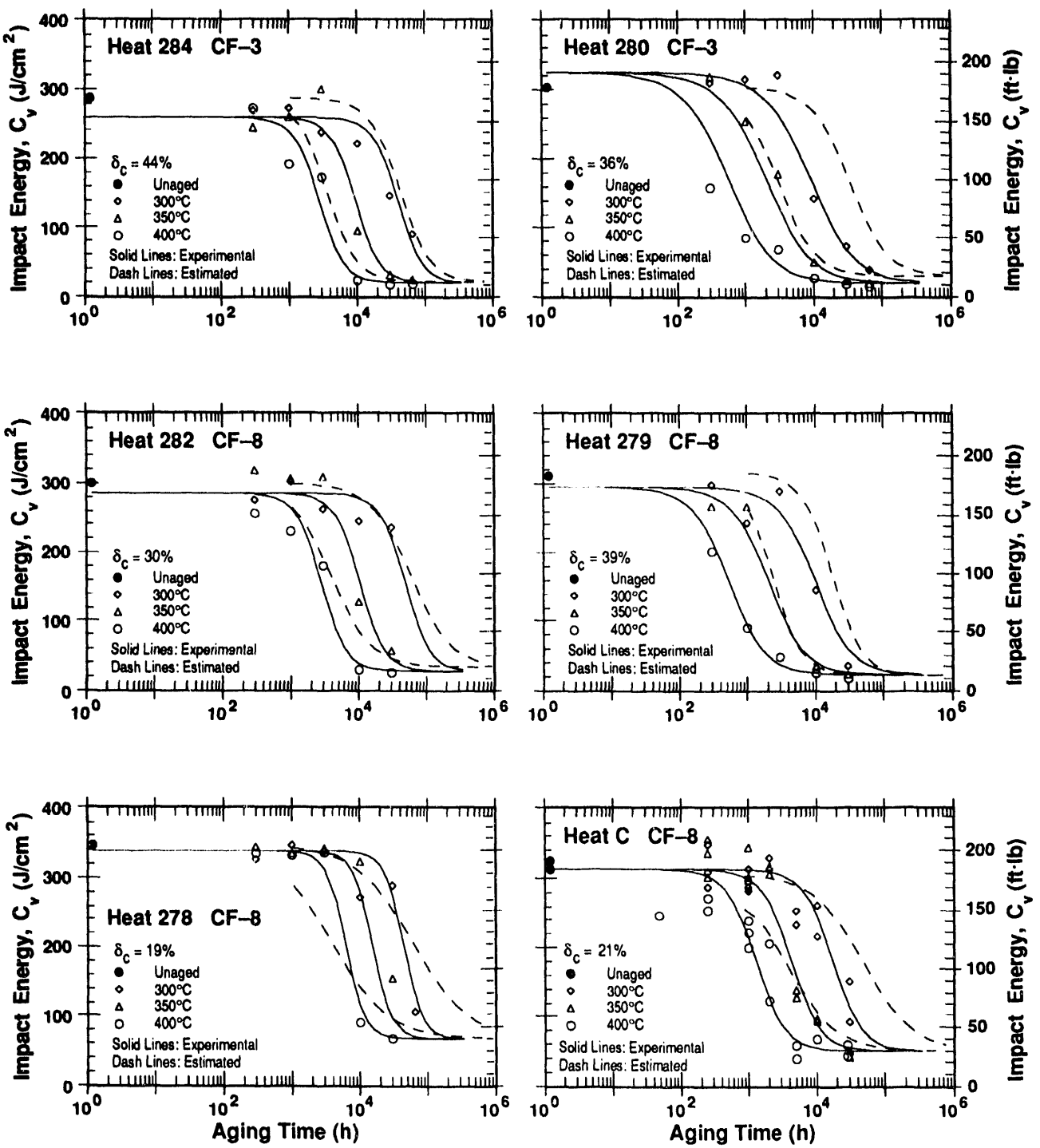

Figure 16. RT Charpy-impact energy for the GF, FRA and EdF heats observed experimentally and estimated from the composition and initial impact energy of the materials. Solid lines represent the best fit of the data at 300, 350, and 400°C and dash lines are the estimates at 300 and 350°C.

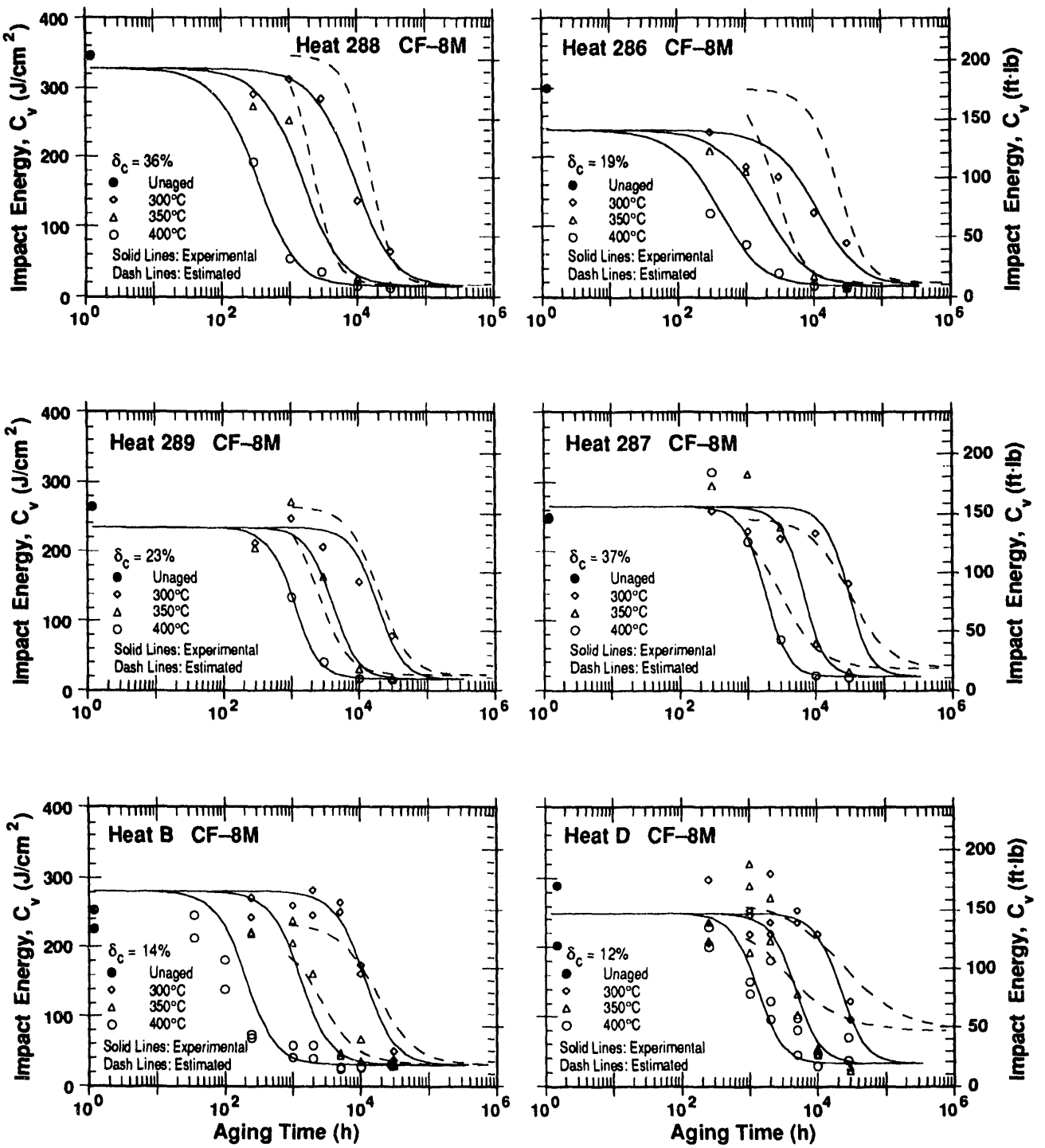

Figure 16. (Contd.)

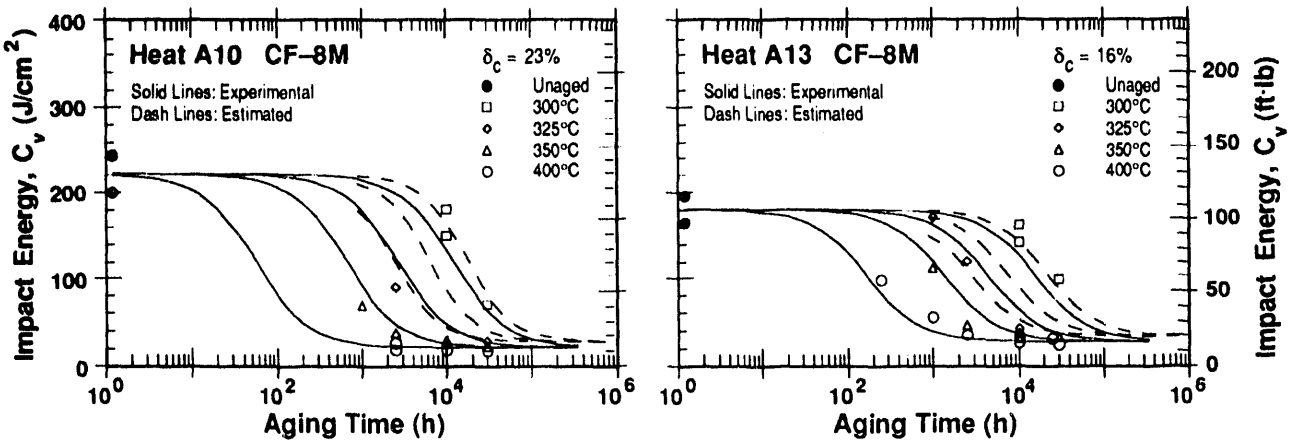

Figure 16. (Contd.)

parameter is normalized with respect to a θ value of 2.9. At both temperatures, the increase in flow stress of CF-3 steels is the smallest and that of CF-8M steels the largest. The tensile-flow-stress ratio $R = (\sigma f_{aged}/\sigma f_{unaged})$ is given by

$$R = a_1 + b_1(P - \theta + 2.9). \quad (18)$$

Equation 18 is valid when ferrite content is >7% and R values are between 1 and a constant c_1. Values of the constants a_1, b_1, and c_1 for different grades of steel and test temperatures are given in Table 6. Experimental and estimated tensile flow stresses at 290°C (554°F) and at RT for various heats of aged cast stainless steel are shown in Fig. 20. For each heat, the aging parameter and activation energy were obtained from Eqs. 14 and 17; because most of the data are for aging temperatures ≥350°C, the actual experimental value of θ was used for all the heats. Tensile flow stress was then estimated from Eq. 18 and the initial flow stress of the materials. The estimated values are within 15% of the observed value for most material and aging conditions.

The fracture toughness J_{IC} values for aged cast stainless steels can be determined from the estimated J-R curve and flow stress. The experimental and estimated J_{IC} for the various heats aged at temperatures ≤350°C are shown in Fig. 21. The chemical composition and the initial Charpy-impact energy and flow stress of the unaged material were used for the estimations. The estimated J_{IC} values show good agreement with the experimental results; for most cases the estimated J_{IC} is lower but within 30% of the observed value.

Table 6. Values of the constants in Eq. 18 for estimating tensile flow stress of aged cast stainless steels

Grade	Room Temp.			290-320°C		
	a_1	b_1	c_1	a_1	b_1	c_1
CF-3	0.94	0.047	1.10	0.89	0.059	1.08
CF-8	0.90	0.074	1.16	0.87	0.088	1.14
CF-8M	0.80	0.101	1.19	0.71	0.143	1.24

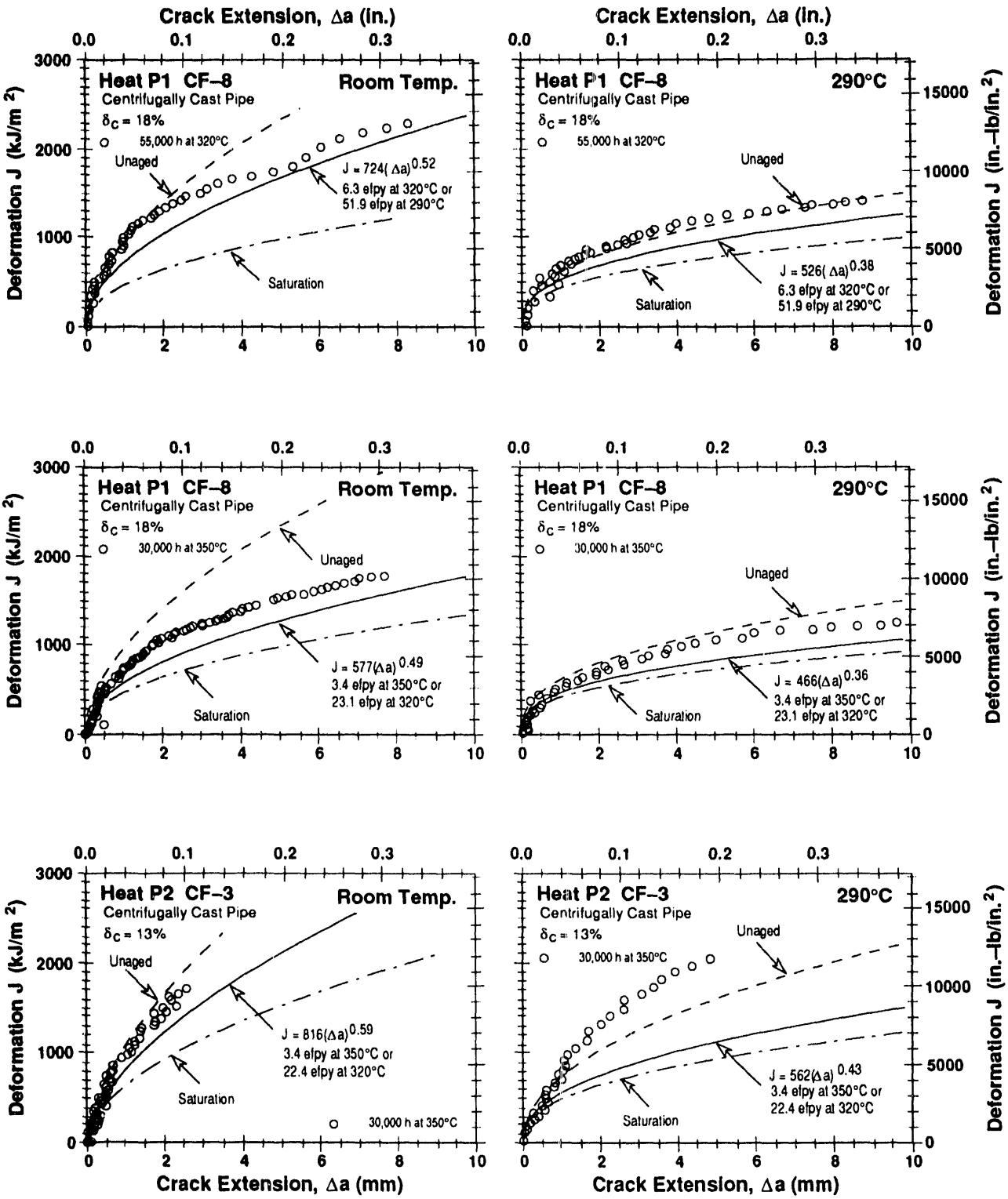

Figure 17. Fracture toughness J-R curve at RT and 290°C, estimated from the chemical composition and initial Charpy-impact energy and determined experimentally for partially aged centrifugally cast CF-3 and CF-8 pipes

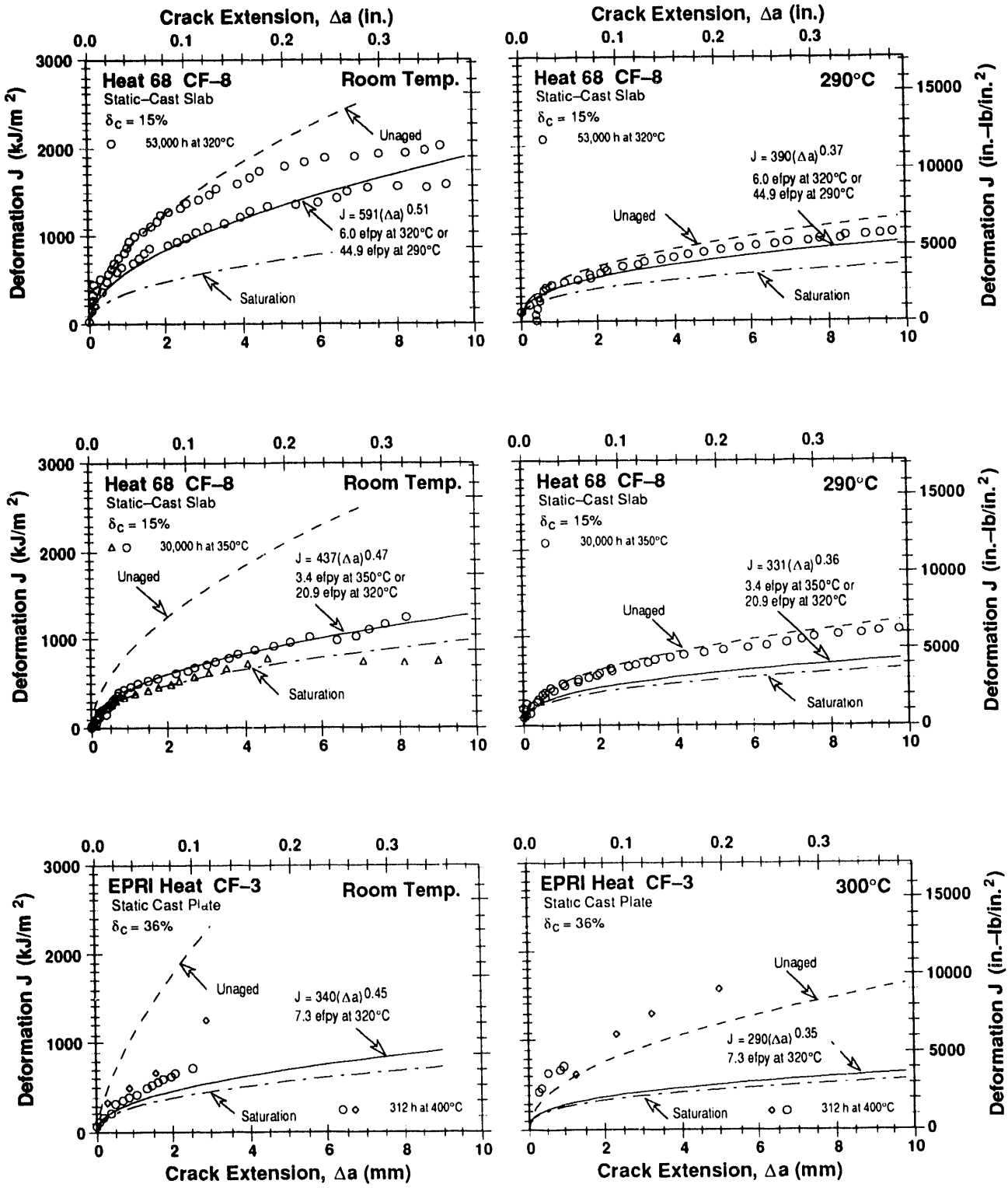

Figure 18. Fracture toughness J–R curves at RT and 290°C, estimated from the chemical composition and initial Charpy–impact energy and determined experimentally for partially aged static–cast CF–3, CF–8, and CF–8M steels

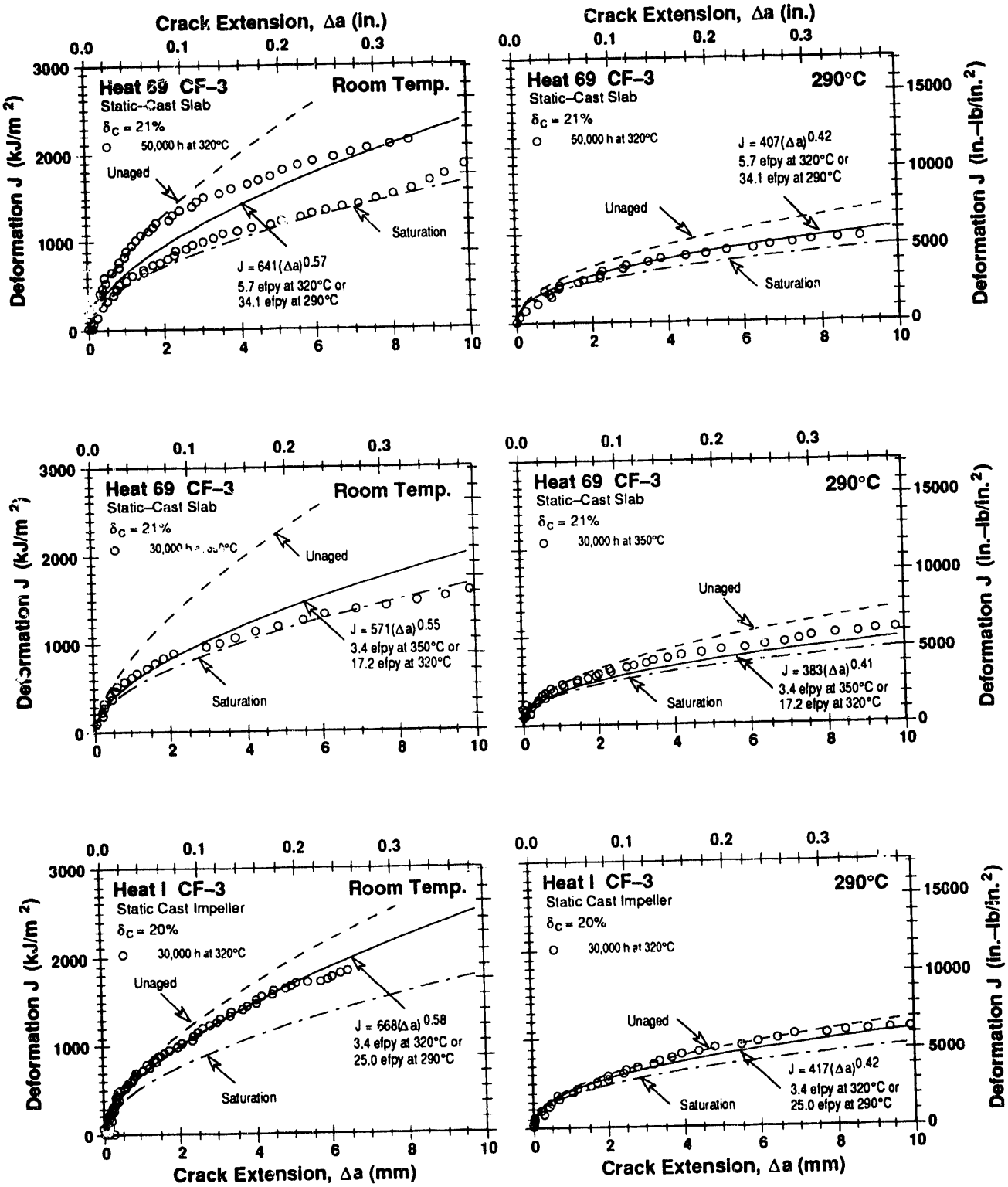

Figure 18. (Contd.)

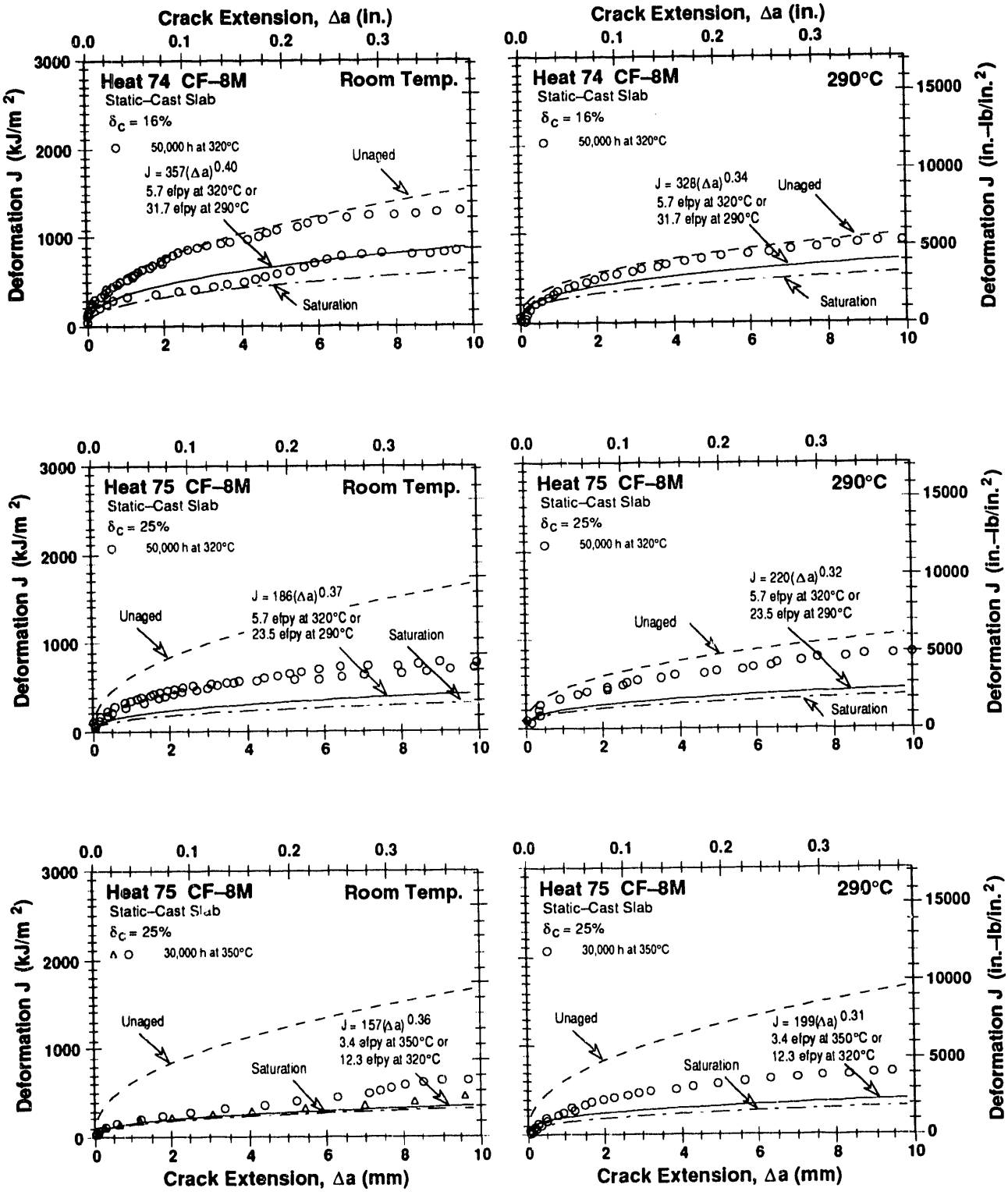

Figure 18. (Contd.)

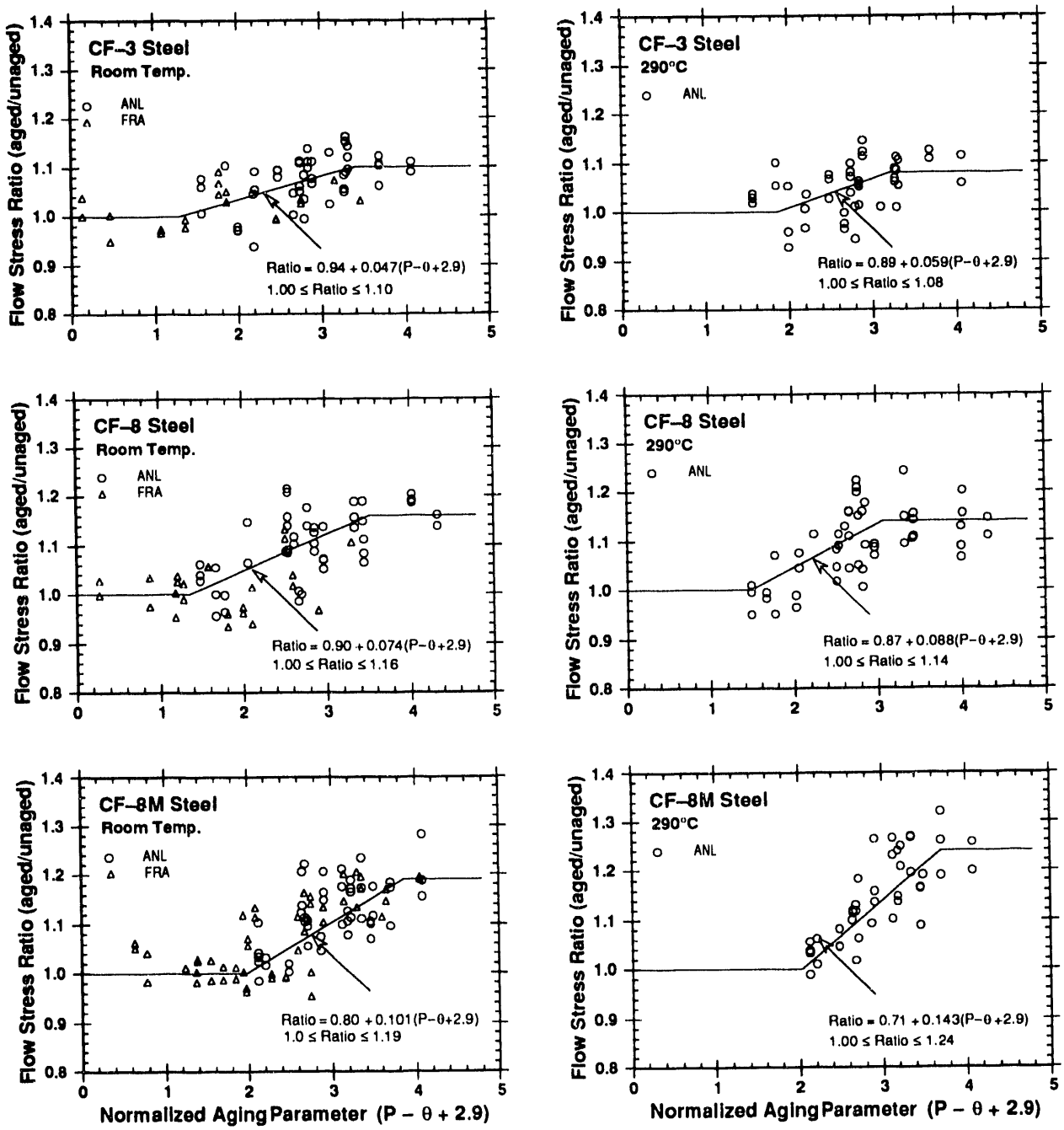

Figure 19. Flow stress ratio of aged cast stainless steels at room temperature and 290°C as a function of normalized aging parameter

4 Conclusions

A procedure and correlations are presented for predicting Charpy-impact energy, tensile flow stress, fracture toughness J-R curve, tearing modulus, and J_{IC} value of aged cast stainless steels (ASTM A 351) from known material information. Mechanical properties of a specific cast stainless steel are estimated from the extent and kinetics of thermal embrittlement.

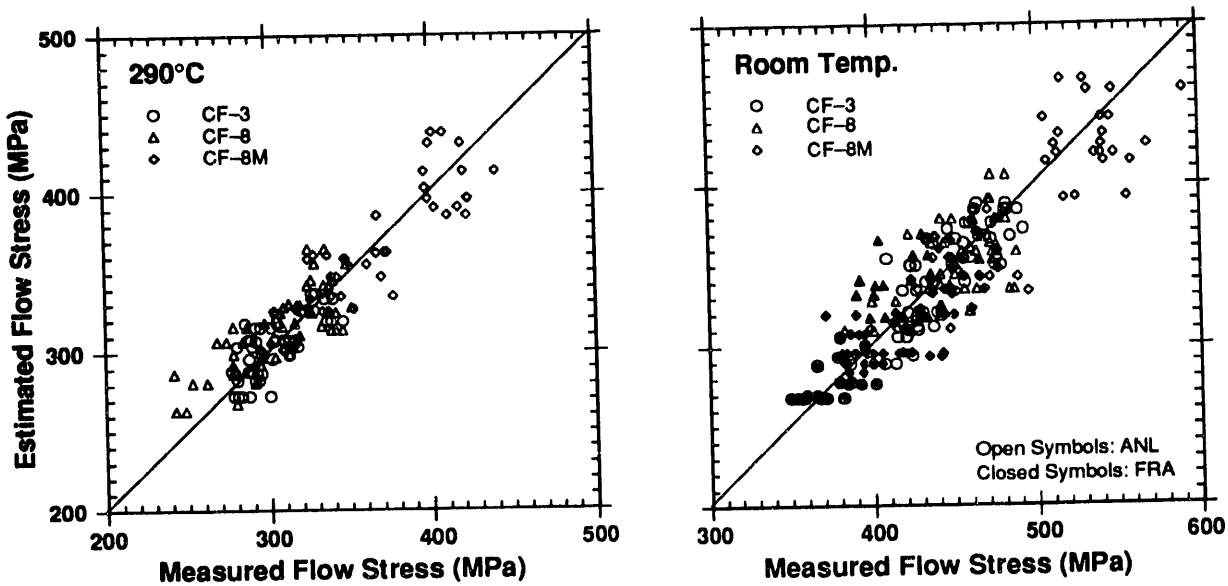

Figure 20. Experimental and estimated flow stress of aged cast stainless steel at 290°C and RT

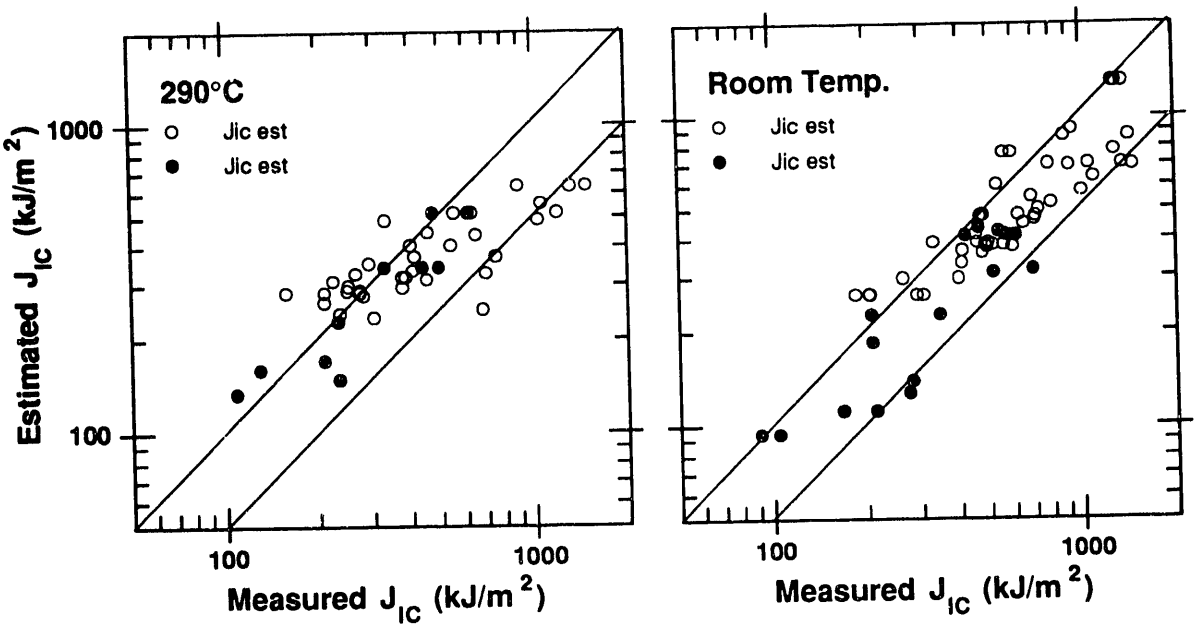

Figure 21. Experimental and estimated values of J_{IC} for aged cast stainless steels

Embrittlement of cast stainless steels is characterized in terms of RT Charpy-impact energy. The extent or degree of thermal embrittlement at "saturation," i.e., the minimum impact energy that can be achieved for a material after long-term aging, is determined from the chemical composition of the steel. A screening criterion is used with the saturation fracture properties to determine whether a detailed assessment of thermal embrittlement is required for the material. Charpy-impact energy as a function of time and temperature of reactor service is estimated from the kinetics of thermal embrittlement, which is also determined from the chemical composition. The initial impact energy of the unaged steel is required for these estimations.

Initial tensile flow stress is needed for estimating the flow stress of the aged material. The fracture toughness J-R curve for the material is then obtained from correlations between RT Charpy-impact energy and fracture toughness parameters. The value of J_{IC} is determined from the estimated J-R curve and flow stress. A common "predicted lower-bound" J-R curve for cast stainless steels with unknown chemical composition is also defined for a given grade of steel, range of ferrite content, and temperature.

Acknowledgments

This work was supported by the Office of the Nuclear Regulatory Research in the U.S. Nuclear Regulatory Commission. The author is grateful to T. M. Galvin, A. Sather, W. F. Michaud, and W. F. Burke for their contributions to the experimental effort. The author also thanks J. Muscara, W. J. Shack, and T. F. Kassner for their helpful discussions.

References

1. O. K. Chopra and H. M. Chung, "Aging Degradation of Cast Stainless Steels: Effects on Mechanical Properties," in *Environmental Degradation of Materials in Nuclear Power Systems-Water Reactors*, G. J. Theus and J. R. Weeks, eds., The Metallurgical Society, Warrendale, PA., pp. 737-748 (1988).

2. O. K. Chopra and H. M. Chung, "Effect of Low-Temperature Aging on the Mechanical Properties of Cast Stainless Steels," in *Properties of Stainless Steels in Elevated Temperature Service*, M. Prager, ed., MPC Vol. 26, PVP Vol. 132, ASME, New York, pp. 79-105 (1988).

3. O. K. Chopra, "Thermal Aging of Cast Stainless Steels: Mechanisms and Predictions," in *Fatigue, Degradation, and Fracture - 1990*, W. H. Bamford, C. Becht, S. Bhandari, J. D. Gilman, L. A. James, and M. Prager, eds., MPC Vol. 30, PVP Vol. 195, ASME, New York, pp. 193-214 (1990).

4. O. K. Chopra and A. Sather, *Initial Assessment of the Mechanisms and Significance of Low-Temperature Embrittlement of Cast Stainless Steels in LWR Systems*, NUREG/CR-5385, ANL-89/17 (August 1990).

5. O. K. Chopra, A. Sather, and L. Y. Bush, *Long-Term Embrittlement of Cast Duplex Stainless Steels in LWR Systems: Semiannual Report, April-September 1989*, NUREG/CR-4744, Vol. 4, No. 2, ANL-90/49 (June 1991).

6. O. K. Chopra, *Long-Term Embrittlement of Cast Duplex Stainless Steels in LWR Systems: Semiannual Report, October 1990-March 1991*, NUREG/CR-4744, Vol. 6, No. 1, ANL-91/22 (August 1992).

7. O. K. Chopra, *Long-Term Embrittlement of Cast Duplex Stainless Steels in LWR Systems: Semiannual Report, October 1991-March 1992*, NUREG/CR-4744, Vol. 7, No. 1, ANL-92/42 (April 1993).

8. O. K. Chopra, "Evaluation of Aging Degradation of Structural Components," in *Proceedings of the Aging Research Information Conference*, NUREG/CP-0122, Vol. 2, pp. 369-386 (1992).

9. O. K. Chopra, *Estimation of Fracture Toughness of Cast Stainless Steels during Thermal Aging in LWR Systems*, NUREG/CR-4513, ANL-90/42 (June 1991).

10. O. K. Chopra, "Thermal Aging of Cast Stainless Steels in LWR Systems: Estimation of Mechanical Properties," in *Nuclear Plant Systems/Components Aging Management and Life Extension*, I. T. Kisisel, J. Sinnappan, R. W. Carlson, and W. H. Lake eds., PVP Vol. 228, ASME, New York, pp. 79-92 (1992).

11. O. K. Chopra, "Prediction of Aging Degradation of Cast Stainless Steel Components in LWR Systems," in *Proceedings of the Aging Research Information Conference*, NUREG/CP-0122, Vol. 2, pp. 324-340 (1992).

12. H. M. Chung and O. K. Chopra, "Kinetics and Mechanism of Thermal Aging Embrittlement of Duplex Stainless Steels," in *Environmental Degradation of Materials in Nuclear Power Systems-Water Reactors*, G. J. Theus and J. R. Weeks, eds., The Metallurgical Society, Warrendale, PA, pp. 359-370 (1988).

13. H. M. Chung and O. K. Chopra, "Long-Term Aging Embrittlement of Cast Austenitic Stainless Steels - Mechanism and Kinetics," in *Properties of Stainless Steels in Elevated Temperature Service*, M. Prager, ed., MPC Vol. 26, PVP Vol. 132, ASME, New York, pp. 17-34 (1988).

14. H. M. Chung and T. R. Leax, "Embrittlement of Laboratory and Reactor Aged CF3, CF8, and CF8M Duplex Stainless Steels," *Mater. Sci. Technol.*, **6**, 249-262 (1990).

15. A. Trautwein and W. Gysel, "Influence of Long Time Aging of CF-8 and CF-8M Cast Steel at Temperatures Between 300 and 500°C on the Impact Toughness and the Structure Properties," in *Spectrum, Technische Mitteilungen aus dem+GF+Konzern, No. 5* (May 1981); also in *Stainless Steel Castings*, V. G. Behal and A. S. Melilli, eds., STP 756, ASTM, Philadelphia, PA., pp. 165-189 (1982).

16. E. I. Landerman and W. H. Bamford, "Fracture Toughness and Fatigue Characteristics of Centrifugally Cast Type 316 Stainless Steel Pipe after Simulated Thermal Service Conditions," in *Ductility and Toughness Considerations in Elevated Temperature Service*, MPC 8, ASME, New York, pp. 99-127 (1978).

17. S. Bonnet, J. Bourgoin, J. Champredonde, D. Guttmann, and M. Guttmann, "Relationship between Evolution of Mechanical Properties of Various Cast Duplex Stainless Steels and Metallurgical and Aging Parameters: An Outline of Current EDF Programmes," *Mater. Sci. Technol.*, **6**, 221-229 (1990).

18. P. H. Pumphrey and K. N. Akhurst, "Aging Kinetics of CF3 Cast Stainless Steel in Temperature Range 300-400°C," *Mater. Sci. Technol.*, **6**, 211-219 (1990).

19. G. Slama, P. Petrequin, and T. Mager, "Effect of Aging on Mechanical Properties of Austenitic Stainless Steel Castings and Welds," presented at *SMIRT Post-Conference Seminar 6, Assuring Structural Integrity of Steel Reactor Pressure Boundary Components*, August 29–30, 1983, Monterey, CA.

20. Y. Meyzaud, P. Ould, P. Balladon, M. Bethmont, and P. Soulat, "Tearing Resistance of Aged Cast Austenitic Stainless Steel," presented at *Int. Conf. on Thermal Reactor Safety (NUCSAFE 88)*, October 1988, Avignon, France.

21. P. McConnell and J. W. Sheckherd, *Fracture Toughness Characterization of Thermally Embrittled Cast Duplex Stainless Steel*, Report NP-5439, Electric Power Research Institute, Palo Alto, CA (September 1987).

22. G. E. Hale and S. J. Garwood, "The Effect of Aging on the Fracture Behaviour of Cast Stainless Steel and Weldments," *Mater. Sci. Technol.*, **6**, 230–235 (1990).

23. P. Auger, F. Danoix, A. Menand, S. Bonnet, J. Bourgoin, and M. Guttmann, "Atom Probe and Transmission Electron Microscopy Study of Aging of Cast Duplex Stainless Steels," *Mater. Sci. Technol.*, **6**, 301–313 (1990).

24. M. Vrinat, P. Cozar, and Y. Meyzaud, "Precipitated Phases in the Ferrite of Aged Cast Duplex Stainless Steels," *Scripta Metall.*, **20**, 1101–1106 (1986).

25. P. Joly, R. Cozar, and A. Pineau, "Effect of Crystallographic Orientation of Austenite on the Formation of Cleavage Cracks in Ferrite in an Aged Duplex Stainless Steel," *Scripta Metall.*, **24**, 2235–2240 (1990).

26. J. M. Sassen, M. G. Hetherington, T. J. Godfrey, and G. D. W. Smith, "Kinetics of Spinodal Reaction in the Ferrite Phase of a Duplex Stainless Steel," in *Properties of Stainless Steels in Elevated Temperature Service*, M. Prager, ed., MPC Vol. 26, PVP Vol. 132, ASME, New York, pp. 65–78 (1988).

27. J. E. Brown, A. Cerezo, T. J. Godfrey, M. G. Hetherington, and G. D. W. Smith, "Quantitative Atom Probe Analysis of Spinodal Reaction in Ferrite Phase of Duplex Stainless Steel," *Mater. Sci. Technol.*, **6**, 293–300 (1990).

28. M. K. Miller, and J. Bentley, "Characterization of Fine-Scale Microstructures in Aged Primary Coolant Pipe Steels," in *Environmental Degradation of Materials in Nuclear Power Systems-Water Reactors*, G. J. Theus and J. R. Weeks, eds., The Metallurgical Society, Warrendale, PA., pp. 341–349 (1988).

29. O. K. Chopra and L. Y. Bush, *Long-Term Embrittlement of Cast Duplex Stainless Steels in LWR Systems: Semiannual Report October 1989–March 1990*, NUREG/CR-4744, Vol. 5, No. 1, ANL-91/7 (July 1991).

30. A. W. Bowen and G. M. Leak, "Diffusion in BCC Iron Base Alloys," *Metall. Trans.*, **1**, 2767 (1970).

31. L. S. Aubrey, P. F. Wieser, W. J. Pollard, and E. A. Schoefer, "Ferrite Measurement and Control in Cast Duplex Stainless Steel," in *Stainless Steel Castings*, V. G. Behal and A. S. Melilli, eds., STP 756, ASTM, Philadelphia, PA., pp. 126–164 (1982).

32. A. L. Hiser, *Fracture Toughness Characterization of Nuclear Piping Steels*, NUREG/CR-5118, MEA-2325, Materials Engineering Associates, Inc. (November 1989).

33. G. M. Wilkowski, et al., *Degraded Piping Program – Phase II*, Semiannual Report, NUREG/CR-4082, Vol. 2 (June 1985).

34. W. J. Mills, "Heat-to-Heat Variations in the Fracture Toughness of Austenitic Stainless Steels," *Eng. Fracture Mech.*, ***30***, 469–492 (1988).

35. M. G. Vass Iaros, R. A. Hays, and J. P. Gudas, "Investigation of the Ductile Fracture Properties of Type 304 Stainless Steel Plate, Welds, and 4-Inch Pipe," in *Proc. 12th Water Reactor Safety Information Meeting*, U.S. Nuclear Regulatory Commission, NUREG/CP-0058, Vol. 4, p. 176 (January 1985).

36. P. Balladon, J. Heritier, and P. Rabbe, "Influence of Microstructure on the Ductile Rupture Mechanisms of a 316L Steel at Room and Elevated Temperatures," in *Fracture Mechanics: Fourteenth Symposium*, STP 791, ASTM, Philadelphia, PA., pp. II496–II513 (1983).

37. W. H. Bamford and A. J. Bush, "Fracture Behavior of Stainless Steel," *Elastic-Plastic Fracture*, STP 668, ASTM, Philadelphia, PA, pp. 553–577 (1979).

Distribution for NUREG/CR-4744 Vol. 7, No. 2 (ANL-93/11)

Internal:

O. K. Chopra (25)
H. M. Chung
T. F. Kassner
C. Malefyt (2)
R. B. Poeppel
W. J. Shack
C. E. Till
R. W. Weeks
TIS Files

External:

NRC, for distribution per R5
ANL Libraries
ANL-E
ANL-W
Manager, Chicago Field Office, DOE
Energy Technology Division Review Committee
H. K. Birnbaum, University of Illinois, Urbana, IL
R. C. Buchanan, University of Cincinnati, Cincinnati, OH
M. S. Dresselhaus, Massachusetts Institute of Technology, Cambridge, MA
B. G. Jones, University of Illinois, Urbana, IL
C.-Y. Li, Cornell U., Ithaca, NY
S.-N. Liu, Electric Power Research Institute, Palo Alto, CA
R. E. Smith, Engineering Applied Sciences, Inc., Trafford, PA
D. Atteridge, Battelle Pacific Northwest Laboratory
W. H. Bamford, Westinghouse Electric Corp., Pittsburgh
N. G. Cofie, Nutech, San Jose, CA
A. Cowan, Risley Nuclear Power Development Labs., Risley, Warrington, UK
E. L. Creamer, Shell Oil Co., Houston
W. H. Cullen, Materials Engineering Associates, Inc., Lanham, MD
B. J. L. Darlaston, Berkeley Nuclear Laboratories, Berkeley, Gloucestershire, UK
H. Domian, Alliance Research Center, Babcock & Wilcox Co., Alliance, OH
G. Gage, AEA Technology, Harwell Laboratory, Oxfordshire, UK
J. Gilman, Electric Power Research Inst., Palo Alto, CA
M. Guttmann, Electricité de France, Les Renardieres Roule de Sens, France
W. Gysel, Georg Fischer, Ltd., Schaffhausen, Switzerland
G. E. Hale, The Welding Institute, Abington, Cambridge, UK
P. Hedgecock, APTECH Engineering Services, Inc., Palo Alto, CA
B. Hemsworth, HM Nuclear Installations Inspectorate, London
C. G. Interrante, Center for Materials Science, National Institute of Standards and Technology, Gaithersburg, MD
J. Jansky, Buro für Technische Beratung, Leonberg, Germany
C. E. Jaske, CC Technologies, Cortest, Columbus, OH
C. Kim, Westinghouse Electric Corp., Pittsburgh
P. M. Lang, Office of Converter Reactor Deployment, U.S. Dept. of Energy, Washington, DC
G. J. Licina, Structural Integrity Associates, San Jose, CA
T. R. Mager, Westinghouse Electric Corp., Pittsburgh
Y. Meyzaud, Framatome, Paris La Defense, France

M. Prager, Materials Properties Council, Inc., New York
P. H. Pumphrey, National Power, Technology and Environment Center, Leatherhead, Surrey, UK
D. Quiñones, Robert Cloud & Associates, Berkeley, CA
V. N. Shah, EG&G Idaho, Inc., Idaho Falls, Idaho
V. K. Sikka, Oak Ridge National Laboratory
A. Singh, Unical Science & Technology Division, Brea, CA
G. Slama, Framatome, Paris La Defense, France
G. D. W. Smith, Oxford University, Oxford, UK
H. D. Solomon, General Electric Co., Schenectady, NY
D. M. Stevens, Lynchburg Research Center, Babcock & Wilcox Co., Lynchburg, VA
L. Taylor, Nuclear Electric plc., Chelsford Rd., Knutsford, Cheshire, UK
J. M. Vitek, Oak Ridge National Laboratory
J. Wilks, AMOCO, Naperville, IL

DATE
FILMED
9/22/93

END